Food and Chemical Toxicology 125 (2019) 252–270

Contents lists available at ScienceDirect

Food and Chemical Toxicology

journal homepage: www.elsevier.com/locate/foodchemtox

Assessment of a 72-hour repeated exposure to Swedish snus extract and total particulate matter from 3R4F cigarette smoke on gingival organotypic cultures

Filippo Zanetti[a,*], Alain Sewer[a], Bjoern Titz[a], Walter K. Schlage[b], Anita R. Iskandar[a], Athanasios Kondylis[a], Patrice Leroy[a], Emmanuel Guedj[a], Keyur Trivedi[a], Ashraf Elamin[a], Florian Martin[a], Stefan Frentzel[a], Nikolai V. Ivanov[a], Manuel C. Peitsch[a], Julia Hoeng[a]

[a] PMI R&D, Philip Morris Products S.A., Quai Jeanrenaud 5, CH-2000 Neuchâtel, Switzerland
[b] Biology Consultant, Max-Baermann-Str. 21, 51429 Bergisch Gladbach, Germany

ARTICLE INFO

Keywords:
Cigarette smoke
Oral health
Swedish snus
Systems toxicology
Air-liquid interface
Smokeless tobacco product

ABSTRACT

Swedish snus is a smokeless tobacco product that contains reduced levels of harmful compounds compared with cigarette smoke. In Sweden, where snus use exceeds smoking among men, relatively low rates of major smoking-related diseases have been recorded. To better understand how snus use could align with current tobacco harm reduction strategies, its potential mechanisms of toxicity must be investigated.

This study aimed to determine, via a systems toxicology approach, the biological impact of repeated 72-hour exposure of human gingival epithelial organotypic cultures to extracts from both a commercial and a reference snus and the total particulate matter (TPM) from cigarette smoke. At concentrations relevant for human use, cultures treated with snus extracts induced mild, generally reversible biological changes, while TPM treatment induced substantial morphological and inflammatory alterations. Network enrichment analysis and integrative analysis of the global mRNA and miRNA expression profiles indicated a limited and mostly transient impact of the snus extracts, in particular on xenobiotic metabolism, while the effects of TPM were marked and sustained over time. High-confidence miRNAs that might be related to pathological conditions *in vivo* were identified.

This study highlights the limited biological impact of Swedish snus extract on human organotypic gingival cultures.

1. Introduction

Swedish snus is a type of moist snuff, an air-cured, heat-pasteurized oral smokeless tobacco product (STP), widely used in Sweden. Snus is generally used in form of 1-g pouches, which are placed between the gingiva and upper lip, often for 11–14 h daily (IARC, 2007). Exposure to nicotine in snus users is similar or even greater than that from smoking (Holm et al., 1992). Compared with other Western European countries, Sweden shows a lower rate of manufactured cigarette smoking in males. In addition, Sweden exhibits a relatively low rate of major smoking-related diseases compared to other European and non-European countries (Foulds et al., 2003; Lee, 2011).

The tobacco harm reduction strategy, which was defined by the Institute of Medicine (IoM) as “decreasing total morbidity and mortality, without the complete elimination of tobacco and nicotine use”, is aimed at decreasing smoking and hence smoking-related population harm (Stratton et al., 2001). According to the IoM, products that provide a reduction in exposure to one or more tobacco constituents are part of this strategy. As the tobacco in snus is not burned, and its specific manufacturing process does not involve fermentation, snus has significantly lower levels of harmful and potentially harmful constituents (HPHC). For example, the carcinogenic tobacco-specific nitrosamines (TSNAs) are lower than the TSNAs in cigarette smoke and in other STPs, such as American moist snuff (IARC, 2007; Seidenberg et al., 2016).

A substantial number of studies provided conflicting evidence on the adverse effects of snus use on oral health, mainly due to confounding factors in epidemiological data, specific data selection for meta-analyses, and lack of distinction between oral tobacco products with widely varying composition (Bergstrom et al., 2006; Carlens et al., 2010; Gustafsson et al., 2011; Kallischnigg et al., 2008; Lee, 2013a, 2013b; Modeer et al., 1980; Persson et al., 1993, 2000). *In vitro* studies

* Corresponding author. PMI R&D, Philip Morris Products S.A., Quai Jeanrenaud 5, CH-2000 Neuchâtel, Switzerland.
E-mail address: filippo.zanetti@pmi.com (F. Zanetti).

https://doi.org/10.1016/j.fct.2018.12.056
Received 20 September 2018; Received in revised form 11 December 2018; Accepted 30 December 2018
Available online 02 January 2019

Abbreviations

2D	Two-dimensional
3D	Three-dimensional
3R4F	Reference cigarette
BIF	Biological impact factor
cDNA	Complementary DNA
CFA	Cell fate
CPR	Cell proliferation
CRP1.1	CORESTA Reference Product 1.1
cRNA	Complementary RNA
CSF	Colony stimulating factor
CST	Cell stress
CXCL	Chemokine (C-X-C motif) ligand
DEG	Differentially expressed genes
EtOH	Ethanol
FC	Fold change
FDR	False discovery rate
GCW	General Classic White snus
GSA	Gene set analysis
H&E	Hematoxylin and eosin
HPHC	Harmful and potentially harmful constituents
IFNγ	Interferon gamma
IL	Interleukin
IoM	Institute of Medicine
IPN	Inflammatory process network
KEGG	Kyoto Encyclopedia of Genes and Genomes
LC	Liquid chromatography
miRNA	MicroRNA
MMP	Matrix metalloproteinase
mRNA	Messenger RNA
MRTP	Modified risk tobacco product
MS	Mass spectrometry
NA	Not applicable
NAB	N-Nitrosoanabasine
NAT	N-Nitrosoanatabine
NNN	N-Nitrosonornicotine
NNK	4-(N-nitrosomethylamino)-1-(3-pyridyl)-1-butanone
NPA	Network perturbation amplitude
NUSE	Normalized-unscaled standard errors
PBS	Phosphate-buffered saline
PE	Post-exposure
PRM	Parallel reaction monitoring
QC	Quality control
RBIF	Relative biological impact factor
REF	Reference
RLE	Relative log expressions
RT	Room temperature
SEM	Standard error of the mean
sICAM-1	Soluble intercellular adhesion molecule-1
STE	Smokeless tobacco extract (American-type reference moist snuff)
STP	Smokeless tobacco product
TIMP-1	Tissue inhibitor of metalloproteinases-1
TNFA	Tumor necrosis factor alpha
TPM	Total particulate matter
TSNA	Tobacco-specific nitrosamine
VEGF	Vascular endothelial growth factor
WS	Whole smoke

performed by administering snus extracts to cell cultures have shown only weak adverse effects of snus at concentrations relevant for human use. Swedish snus was broadly showing negative results in the Salmonella reverse mutation (Ames), mouse lymphoma mutagenicity, and *in vitro* micronucleus assays, whereas an American-type reference product was weakly positive (Coggins et al., 2012). Acute exposure (1 h) of primary human endothelial cells and oral fibroblasts to high concentrations (100 μM nicotine) of Swedish snus extract or nicotine alone (up to 400 μM) induced abnormalities in the cytoplasm without any significant degree of cell death; some gene expression changes were observed on a complementary DNA (cDNA) array of 100 selected genes, displaying diverse responses between both cell types (Laytragoon-Lewin et al., 2011). In a comparative study on Sudanese toombak versus Swedish snus, oral fibroblasts and keratinocytes exposed to snus displayed less impairment of cell viability, morphology, growth, senescence, and DNA double-strand breaks (Costea et al., 2010). Woo et al. investigated the gene expression profiles in normal gingival keratinocytes and tumor-derived oral cell lines following a 24-hour exposure to an extract from an American-type reference STP and observed mainly activation of genes related to xenobiotic metabolism (Woo et al., 2017).

The manufacture of snus products evolved in recent years, leading, for example, to a reduction in TSNA levels (Rutqvist et al., 2011). Therefore, effects such as cellular damage, impairment of cell cycle, and cell death observed in previous studies may not reflect the effects reported in more recent studies (Coggins et al., 2012).

Most snus *in vitro* studies were performed on two-dimensional (2D), often tumor-derived or immortalized, culture models, which are grown as a monolayer in a non-physiologic medium-submerged environment and do not retain the organization of human tissues. A culture grown to form a three-dimensional (3D) structure is expected to be more relevant than a 2D culture, as it retains many properties of the native tissue (Mulhall et al., 2013). We leveraged these properties of a gingival human epithelial organotypic culture that is made of primary normal human gingival keratinocytes cultured in a serum-free medium, which form 3D differentiated tissues. This tissue structure is very similar to the native human gingival epithelium (Hai et al., 2006; Zanetti et al., 2017). To our knowledge, this is the first study to assess the impact of Swedish snus on fully differentiated gingival organotypic cultures.

Systems toxicology integrates systems biology into toxicity assessment; functional changes are studied as well as alterations in cellular and molecular entities. The essence of a systems toxicology approach is switching from qualitative–descriptive to quantitative–predictive science (Sauer et al., 2016; Sturla et al., 2014). In recent years, we successfully combined a systems toxicology approach with the use of 3D organotypic buccal and gingival cultures to investigate the effects of different tobacco products (Schlage et al., 2014; Zanetti et al., 2016, 2017, 2018).

In the current study, we used systems toxicology to characterize the effects of apical exposure to aqueous snus extracts obtained from a commercially available Swedish snus brand and from a Swedish snus reference product on organotypic gingival epithelial cultures. Three concentrations of each product were tested and matched for their nicotine content, which was considered as internal reference compound. Total particulate matter (TPM) extracted from reference cigarette smoke was used as a positive control and representative smoke fraction to assess the effects of combusted tobacco on gingival cells. The concentrations of secreted inflammatory mediators were measured and culture morphology was investigated by evaluating the hematoxylin/eosin (H&E)-stained sections and E-cadherin immunostaining. Microarrays were used to obtain gene expression profiles (messenger RNA [mRNA] and microRNA [miRNA]), and computational modeling, including our previously established causal network approach, was conducted to analyze the expression profiles under a mechanistic

context. We also applied our causal network modeling approach to the transcriptomics data set by (Woo et al., 2017), underlining the utility of this tool as well as the robustness of our findings.

2. Materials and methods

2.1. Organotypic culture model

Human gingival organotypic epithelial cultures (EpiGingival™, GIN-100) were purchased from MatTek (Ashland, MA, USA). Gingival cultures were derived from a 46-year-old nonsmoker male donor with no reported pathologies and were handled and maintained as described previously (Zanetti et al., 2017). Briefly, the cells were grown in Transwell® inserts (with a diameter of 6.5 mm and a pore size of 0.4 µm) and maintained in 12-well culture plates for three days to complete differentiation at the air-liquid interface. After differentiation, cultures were incubated in 24-well plates.

2.2. Tobacco product preparations

Swedish snus extracts were obtained from the CORESTA Reference Product 1.1 (CRP1.1, Tobacco Analytical Services Laboratory, North Carolina State University, Raleigh, NC, USA) or the General Classic White (GCW, Swedish Match, Stockholm, Sweden). Upon receipt, CRP1.1 and GCW packages were stored at −20 °C. The snus boxes were placed at +4 °C for a minimum of 24 h prior to the experiments. One hour before the extraction, snus pouches were placed at room temperature (RT) to equilibrate. Five snus pouches of each type were cut in half, and the pouch material and content (5 g) were extracted with 25 mL PBS (1/5 dilution) for 1 h at 37 °C under agitation (400 rpm). The extract was then centrifuged at 2500 rpm for 5 min at RT, and the supernatant was subsequently centrifuged into a second centrifuge tube equipped with a centrifuge glass filter (Labo Service Belgium bvba, Kontich, Belgium). The glass filter was protected with an F44 mm glass-fiber filter pad (0.45 µm pore size syringe filer, Fisher Scientific, Waltham, MA, USA) and the extract was centrifuged for 10 min at 2400 rpm. The centrifuged/pre-filtered extract was filled into a 10-mL glass syringe with a polytetrafluoroethylene head and filtered through a 0.22-µm pore size syringe filter (Fisher Scientific; PES membrane, 33 mm diameter, sterile). The snus preparation obtained were referred to as 100% concentrated. Further dilutions were performed in PBS. PBS was used as solvent control (sham).

TPM was prepared according to a standard procedure by collecting mainstream smoke from 3R4F reference cigarettes (University of Kentucky, Kentucky Tobacco Research and Development Center, Lexington, KY, USA). TPM samples were generated according to the Health Canada Intense smoking protocol (55 mL puff over 1.9 s, twice per min). Each 3R4F cigarette was smoked to a standard butt length (approximately 35 mm) through a RM20H Rotary smoking machine (Borgwaldt, Hamburg, Germany). Two separate glass fiber filters (44 mm diameter) were used for the collection of the TPM. The smoke from three 3R4F cigarettes was trapped per each filter. TPM was extracted from the first glass fiber filter with 5 mL of pure ethanol (99.9%). The second filter was extracted with the first crude extract. Samples were finally shaken for 10 min at 400 rpm. Further dilutions were performed in phosphate-buffered saline (PBS) (for the TPM high concentration) or PBS-2% ethanol (for the TPM low concentration). PBS-2% ethanol was used as solvent control (sham).

2.3. Nicotine determination in snus and TPM extracts

Nicotine content was determined directly in the TPM (extracted in ethanol) and in the snus extract (in PBS) stock solutions. The nicotine concentrations were measured using liquid chromatography (LC) high-resolution accurate-mass mass spectrometry (MS) (MicroTOF QII, Bruker Daltonik GmbH, Bremen, Germany). A high-throughput method in full-scan positive electrospray ionization mode, using reverse-phase mode chromatography, was used to perform the analysis. The determination of nicotine was achieved using an eight-point calibration curve generated by the area ratio between the analyte of interest and its isotopic-labelled internal standard as a function of concentration. Quantification was performed using an isotopic dilution technique with nicotine-(methyl-d3) as internal standard (Zanetti et al., 2017).

2.4. Determination of TSNAs in snus extracts and TPM

Aliquots (50 µL) of the snus extracts or of diluted TPM (1:10 in methanol) were mixed with a solution of isotopically labelled internal standards – 4-(N-nitrosomethylamino)-1-(3-pyridyl)-1-butanone (NNK)-d4, N-nitrosonornicotine (NNN)-d4, N-nitrosoanatabine (NAT)-d4, and N-nitrosoanabasine (NAB)-d4 – each 25 ng/mL in 50 mM Tris-HCl buffer pH 7.5. These diluted samples, and a series of calibration samples containing the same levels of internal standards together with known concentrations of TSNAs, were analyzed using LC/MS on an Ultimate 3000 ultra-high performance liquid chromatography system coupled to a Q-Exactive mass spectrometer (Thermo Fisher Scientific, Santa Clara, CA, USA). Chromatographic separation was performed using an Acquity Ultra Performance Liquid Chromatography® Ethylene Bridged Hybrid™ C18 column (1.7 µm, 150 × 2.1 mm; Waters, Milford, MA, USA); the column temperature was set to 55 °C. Eluents were 10 mM ammonium bicarbonate in water + acetonitrile (5% v/v; eluent A) and methanol (eluent B) applied as a gradient (0 min–6% B; 1 min–6% B; 5 min–100% B; 6 min–100% B; flow: 0.4 mL/min). The injection volume was 6 µL. In these conditions, NNK, NNN, NAT, and NAB were eluted after 3.81, 3.61, 4.32, and 4.22 min, respectively. For MS detection, electrospray ionization was applied with a capillary

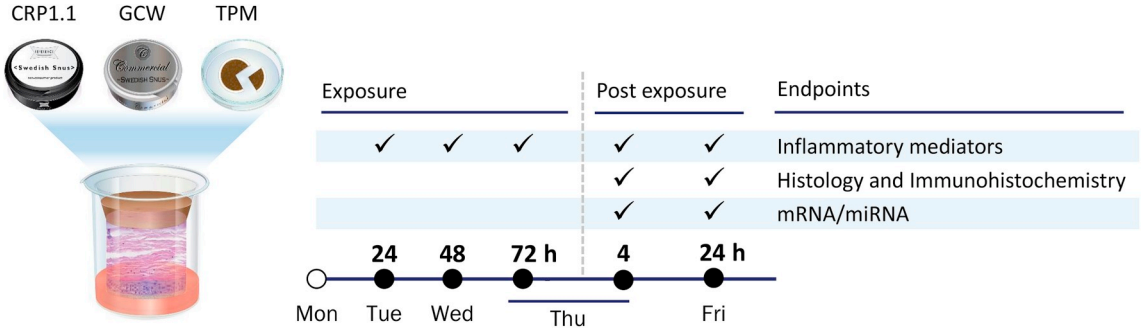

Fig. 1. Scheme of the study design. EpiGingival™ cultures were apically exposed for 72 h to CRP1.1 and GCW extracts, and 3R4F TPM, as described. Basolateral medium for inflammatory mediator assessment was collected (400 µL per sample) at the indicated time points and replaced with fresh medium. Inserts for histological and transcriptomics analysis were collected at the indicated time points. Abbreviations: CRP1.1, CORESTA Reference Product 1.1; GCW, General Classic White; h, hour; PBS, phosphate-buffered saline; PE, post-exposure; TPM, total particulate matter.

voltage of 3.7 V in positive mode, and two functions were acquired: a full-scan function (2.2–4.0 min; 145–220 m/z) and a parallel reaction monitoring (PRM) function (3.9–5.0 min, collision of m/z 183 to 2013 ion with normalized collision energy of 15 V). For the detection of NNK, NNK-d4, NNN, and NNN-d4, the signals of their $[M+H]^+$ pseudomolecular ions at m/z 208.10805, 212.13316, 178.09749, and 182.12260, respectively, in the full-scan mode were used. For the detection of NAT, NAT-d4, NAB, and NAB-d4, the signals of their $[M\text{-}NO + H]^+$ fragment ions at m/z 160.09950, 164.12461, 162.11515, and 166.14026, respectively, in the PRM mode were used.

2.5. Study design

Three independent preparations of CRP1.1, GCW extracts, and 3R4F TPM, were freshly made within the week before each experimental repetition. A series of three experimental repetitions was conducted. For each experimental repetition, three independent exposures with three independently prepared TPM, CRP1.1, and GCW extracts were performed. A pair design was implemented where the exposed samples (to either CRP1.1, GCW extract, and TPM) were exposed together with their corresponding sham controls during a given exposure session. During the week of experiments, EpiGingival™ cultures were subjected to an apical continuous 72-hour exposure to CRP1.1, GCW extracts, TPM, or their corresponding shams. The apical exposure solution was replaced once a day for all inserts. After the 72-hour exposure, the cultures were covered by PBS for a post-exposure (PE) period of up to 24 h. Endpoints were assessed at various time points during exposure or PE to assess the responses of the cultures to CRP1.1, GCW extracts, and TPM (Fig. 1).

2.6. Histology processing and analysis

Histological assessment was performed at 4 and 24 h after the 72-hour exposure to 3R4F TPM, CRP1.1, or GCW extracts. H&E and E-cadherin staining were performed as previously described (Zanetti et al., 2017). Three tissue sections per condition/experimental replicate were stained. Images were acquired at 40 × magnification. Digital images of the H&E-stained sections (acquired with Nanozoomer 2.0 HT Slide Scanner, Hamamatsu, Hamamatsu City, Japan) were assessed independently in a blinded manner by a certified pathologist (Unilabs Independent Histopathology Services, London, UK).

2.7. Luminex-based measurement of secreted inflammatory mediators

Concentrations of secreted inflammatory mediators were measured in the basolateral medium using Luminex® xMAP® technology (Luminex, Austin, TX, USA) with commercially available assay panels (EMD Millipore Corp., Schwalbach, Germany). Basolateral medium samples were collected at 24, 48, and 72 h during exposure, and media were replaced after each sample collection. Single inserts were dedicated to each PE time point (4, 24 h) (e.g. for one insert, the basolateral medium was sampled during exposure and at 4 h PE, and for another insert, the basolateral medium was sampled during exposure and at 24 h PE). For the measurements, the three aliquots collected during exposure were pooled: the pooling was performed as previous experiments using a similar design (Zanetti et al., 2017) with cigarette smoke did not induce marked inflammatory response before the third exposure. The aliquots collected at 4 and 24 h PE were measured independently. The concentration of each inflammatory mediator at 4 and 24 h PE was summed with the respective concentration measured during exposure to determine the cumulative release throughout the experimental session. The following mediators were measured: colony-stimulating factor (CSF) 2, CSF3, chemokine (C-X-C motif) ligand (CXCL) 1, CXCL10, CXCL8, interferon gamma (IFNγ), interleukin (IL)-6, IL-13, IL-1A, IL-1B, matrix metalloproteinase (MMP)-1, MMP-9, soluble intercellular adhesion molecule (sICAM)-1, tissue inhibitor of metalloproteinases-1 (TIMP-1), tumor necrosis factor alpha (TNFA), and vascular endothelial growth factor (VEGF). Briefly, 25 µL of diluted or undiluted sample were used for each detection and analysis was conducted on a Luminex® 200™, or FLEXMAP 3D® reader, equipped with xPONENT® software (Luminex). Three samples were treated for 24 h with TNFA and IL-1B (each at a 10 ng/mL final concentration) in basolateral medium as a positive control. As a negative control, a second set of triplicate samples was treated for 24 h with PBS in basolateral medium. Positive and negative controls were used fresh for each experimental repetition. Whenever measured concentrations fell below the limit of quantitation, a constant value was used (i.e. half of the lower limit of detection).

2.8. RNA/miRNA isolation and data generation

Total RNA, including miRNA, was isolated from gingival cultures collected 4 and 24 h PE as described previously (Zanetti et al., 2018). The RNA integrity number values of the 180 gingival samples (three experimental repetitions) were distributed between 8.9 and 10, indicating a high quality. For the mRNA array, 100 ng of total RNA were reverse-transcribed to cDNA using the Affymetrix® HT 3′-IVT PLUS kit (Thermo Fisher Scientific). The cDNA was labelled and amplified to complementary RNA (cRNA). The fragmented and labelled cRNA was hybridized to GeneChip® Human Genome U133 Plus 2.0 arrays (Thermo Fisher Scientific) in a GeneChip® Hybridization Oven 645 (Thermo Fisher Scientific) according to the manufacturer's instructions. Arrays were rinsed and stained on a GeneChip® Fluidics Station FS450 DX (Thermo Fisher Scientific) using the Affymetrix® GeneChip® Command Console® Software (AGCC software v-3.2, protocol FS450_0001).

For the miRNA array, 200 ng of total RNA containing low-molecular weight RNA were biotinylated using the FlashTag™ Biotin HSR kit (Affymetrix) and hybridized to GeneChip® miRNA 4.0 arrays (Thermo Fisher Scientific) in a GeneChip® Hybridization Oven 645 (Thermo Fisher Scientific) according to the manufacturer's instructions. Arrays were rinsed and stained on a GeneChip® Fluidics Station FS450 DX (Thermo Fisher Scientific) using the Affymetrix® GeneChip® Command Console® Software (AGCC software v-3.2, protocol FS450_0002).

Finally, the arrays were scanned using a GeneChip® Scanner 3000 7G (Thermo Fisher Scientific). Raw images from the scanner were saved as DAT files. The AGCC software automatically gridded the DAT file images and extracted probe cell intensities into the CEL files.

2.9. Preprocessing of the mRNA data

The raw CEL files were processed using software packages from the Bioconductor suite of microarray analysis tools for the R statistical software environment (Huber et al., 2015; R Core Team, 2013). Background correction and frozen-robust multi-array quantile normalization were applied to generate microarray expression values from the 179 arrays that passed the quality controls (QC) (McCall et al., 2010). The QC metrics examined the distributions of the log-intensities, the normalized-unscaled standard errors (NUSE), the relative log expressions (RLE), and the median absolute value RLE, as well as the general aspect of the array pseudo- and raw images, and were obtained using the *affyPLM* package (Brettschneider et al., 2008). Additionally, the Brainarray Custom CDF environment HGU133Plus2_Hs_ENTREZG v16.0 was used for probeset-level summarization (Dai et al., 2005), as previously described (Iskandar et al., 2017a; Zanetti et al., 2017).

2.10. Statistical analysis of mRNA data

For each experimental factor combination (exposure item, concentration, and PE duration), a statistical model to estimate the treatment effects was fitted with the *limma* package (Smyth, 2004). The model included the exposure run identifier as a blocking variable to account for the paired experimental design of exposure (exposed and

sham control, see the Study Design Section). The *p*-values for each treatment effect were adjusted across genes using the Benjamini-Hochberg false discovery rate (FDR) method (Benjamini and Hochberg, 1995). Differentially expressed genes (DEG) were defined as genes with an FDR < 0.05. The mRNA array data were deposited in the ArrayExpress public repository (ID: E-MTAB-7579).

Gene set analysis (GSA) was performed with pathway maps from the Kyoto Encyclopedia of Genes and Genomes (KEGG) knowledge base (Kanehisa et al., 2014). The significance of the gene set enrichment was assessed using a competitive null hypothesis (Q1) as well as a self-contained null hypothesis (Q2) (Ackermann and Strimmer, 2009). Whereas Q1 tests for the significance of genes in the set versus those not in the set, Q2 tests for a significant difference between the conditions. As a consequence, Q2 is more appropriate in the context of comparative toxicity assessment (e.g. to reveal a significant effect on a given gene set compared with sham-exposed controls), while Q1 can highlight gene sets that dominate these responses (Iskandar et al., 2017c). Concretely, the Q1 statistics were calculated with the CAMERA approach (Wu and Smyth, 2012), and the Q2 statistics were calculated with the ROAST approach (Wu et al., 2010), which takes the gene correlation structures into account. Signed means were used as the gene set-level scores, and the statistical significance *p*-values were obtained for two-tailed tests. Finally, the Benjamini-Hochberg adjustment procedure yielded the FDR *p*-values (Benjamini and Hochberg, 1995).

2.11. Network analysis of the mRNA data

While GSA represents the usual way of interpreting mRNA data in terms of pathways enrichments, our Systems Toxicology approach aims at quantifying the exposure-induced changes in the activities of a variety of biological mechanisms using the "reverse-causal reasoning" (Catlett et al., 2013). Specifically, the network perturbation amplitude (NPA) is a network enrichment approach to quantify the treatment-induced effects in terms of the perturbations of biological mechanisms described by causal network models (Martin et al., 2012, 2014). Briefly, the methodology aims to contextualize the treatment effects by combining the alterations in gene expression into differential node values (e.g. one value for each node of a causal network model). The differential node values are determined by fitting procedures inferring the values that best satisfy the directionality of the edges of the network model (e.g. positive or negative signs). NPA scores are associated with a confidence interval accounting for experimental variation, and the associated *p*-values are computed. In addition, companion statistics, called "O" and "K", and their *p*-values are derived to test the specificity of the NPA scores to the biological structure of the network models. A network is considered significantly perturbed by the exposure if the three *p*-values (experimental variation, O, and K) are below 0.05 (Martin et al., 2014). A systems-wide metric for biological impact, the biological impact factor (BIF) (Hoeng et al., 2012; Thomson et al., 2013), summarizes the impact of the exposure on the cellular system into one single number enabling a simple, high-level quantification of the treatment effects across multiple time points. The calculation of the BIF requires the collection of all 28 applicable, hierarchically structured causal network models (Boué et al., 2015) (Supplementary Table 1) and consists of a suitable aggregation of the NPA values of the individual networks (Hoeng et al., 2014).

2.12. Preprocessing of miRNA data

The CEL files were read using the *oligo* package in the Bioconductor suite of microarray analysis tools for the R statistical software environment (Carvalho and Irizarry, 2010; Huber et al., 2015; R Core Team, 2013). QC of the raw data was performed for each experimental repetition using the *arrayQualityMetrics* package (Kauffmann et al., 2009) and based on the following four metrics: the distances between arrays for raw data, the distances between arrays for normalized data, the NUSE, and the array intensity distributions. Arrays that were outliers in at least two of the metrics were discarded. This process was rerun on the remaining arrays until all were accepted (176 out of 180), as previously described (Iskandar et al., 2017a). Normalized probe-level data were obtained by applying robust multi-array normalization and summarized at the probeset level with the median polish method (Bolstad et al., 2003). Using the annotation provided by Affymetrix and the latest miRNA nomenclature according to miRBase v21 (Kozomara and Griffiths-Jones, 2014), only probesets mapping to human miRNAs were kept in the expression matrix. Additionally, only the miRNA probesets with significantly higher intensity values than their matched background probes were considered as "detected" (Affymetrix miRNA QCT Tool, 2011). A *p*-value threshold of 0.001 was chosen to determine the detection calls based on Wilcoxon tests. If a miRNA probeset was detected in more than 75% of the samples in at least one experimental group (exposed or sham control), it was kept for further analysis; otherwise, it was discarded. This process led to final expression matrices containing 533 rows. The miRNA array data are available in the ArrayExpress repository (ID: E-MTAB-7580).

2.13. Statistical analysis of miRNA data

For each experimental factor combination (exposure item, concentration, and PE duration), a submatrix was extracted from the overall expression matrix by selecting only the paired samples matching the factor values as well as the miRNA probesets that were detected in more than 75% of samples of the corresponding two experimental groups. To estimate the treatment effects, the same statistical model as the one used for mRNA data was applied to the submatrix using the *limma* package (Smyth, 2004). Adjusted *p*-values were obtained following multiple testing corrections with the Benjamini-Hochberg FDR (Benjamini and Hochberg, 1995). MicroRNAs below the FDR threshold of 0.05 were considered as differentially expressed.

2.14. Functional analysis of miRNA data

The approach used to functionally analyze the miRNA data is an adaptation of the computational pipeline applied previously (Zanetti et al., 2018). First, the potential miRNA-mRNA interacting pairs were obtained by filtering the mRNA and miRNA differential expression results for the most promising candidates using reasonable criteria (mRNAs: at least one FDR value smaller than 0.05; miRNAs: at least one FDR value smaller than 0.05 together with an absolute fold change (FC) value larger than 0.5 as well as a mean expression value larger than 7; the miRNAs were additionally filtered for high-confidence mature sequences (Kozomara and Griffiths-Jones, 2014)). The corresponding miRNA-mRNA pairs were first selected based on the FC-based Pearson correlation values smaller than −0.5; they were then intersected with the multiple source-based sets of experimentally validated and high-confidence computationally predicted miRNA-mRNA target pairs embarked in the *multiMiR* package (Ru et al., 2014). This first filtering step yielded a total of 163 potential miRNA-mRNA interacting pairs (10 miRNAs and 143 mRNAs). The relevant pathways regulated by the differentially expressed miRNAs were identified based on enrichment calculations for the mRNAs contained in the sets of potential miRNA-mRNA interacting pairs derived in the first step. These calculations were performed using the hypergeometric distribution-based over-representation statistics implemented in the *Piano* package (Varemo et al., 2013). The pathways were taken from the generic MSigDB C2CP collection (1320 gene sets (Liberzon, 2014)) and then restricted to the Reactome subset (674 gene sets), which turned out to be its most biologically insightful non-redundant subset (Liberzon, 2014). The *p*-values were adjusted by the Benjamini-Hochberg procedure (Benjamini and Hochberg, 1995).

2.15. Statistical analysis

Mean and standard error of the mean (SEM) values are reported unless otherwise specified. Comparisons of data from an exposed sample versus its sham control (i.e. the paired sample from the same exposure run) were performed using a paired *t*-test, and the raw *p*-values obtained are reported. Before applying the paired *t*-test to data from secreted inflammatory mediator analyses (Luminex assay), the values were transformed using the natural log transformation.

Statistical analysis was performed using R-3.1.2 on data from Luminex-based measurements of secreted mediators, while R-3.1.2 and Bioconductor 3.0 were used to perform mRNA/miRNA analysis (Gentleman et al., 2004).

Histopathology scores have been attributed to the cultures after their exposure to the study treatments (TPM and snus). Score attributes related to tissue atrophy, parakeratosis, etc. have been given to each tested sample. These were ordinal categorical outcomes taking integer values from 0 (minimum) up to a maximum depending on the attribute. Relative frequencies of these scores were used to describe the histopathological state of the cultures after exposure.

3. Results

3.1. Chemical analysis of the snus and TPM samples

Chemical analyses were performed on the respective stock preparation (100% snus extract and 3R4F TPM) to determine the levels of nicotine and the selected TSNAs, which were considered as representative compounds for exposure calibration (Table 1). The concentrations of nicotine in CRP1.1 and GCW extracts were similar (1477.11 and 1351.73 mg/L PBS, respectively); the nicotine concentration measured in 3R4F TPM was 2533.39 mg/L ethanol. The levels for selected TSNAs were in the low-ng range for CRP1.1 and GCW extracts, with slightly higher values for the GCW than CRP1.1 extracts, and approximately one/two orders of magnitude higher for TPM than for the snus extracts.

The concentrations for the experimental treatments were selected based on measured nicotine and TSNA concentrations. First, the concentrations of CRP1.1 and GCW extracts were selected to achieve target nicotine and TSNA concentrations in the range measured in the saliva of moist snuff users and therefore relevant to the human situation (i.e. 73–1560 mg nicotine/L saliva, maximum 16 μg/L NNK, 3–140 μg/L NNN, and 4–85 μg/L NAT (Hoffmann and Adams, 1981)). These concentrations are indicated in the study as “high” and correspond to a 50% (738.6 mg nicotine/L PBS) and 60% extract solution (811.0 mg nicotine/L PBS) for CRP1.1 and GCW extracts, respectively (Table 2). Second, CRP1.1 and GCW extracts were diluted to yield comparable nicotine concentrations to TPM, which was selected as a positive control treatment to measure morphological/molecular alterations derived from a smoke fraction. A dose range finding experiment was conducted to determine a toxic TPM concentration, which would induce visible morphological alterations to gingival cells, and a lower concentration, which would cause less cellular damage but measurable molecular changes (data not shown). As the nicotine concentration in the 100% TPM preparations was approximatively 1.6-fold higher than that of CRP1.1 and GCW extracts, different dilutions were applied to obtain comparable nicotine concentrations. The two selected TPM dilutions for the study were 0.5% and 2% (12.7 and 50.7 mg nicotine/L PBS, indicated as low and high, respectively [Table 2]), which were comparable to 1% and 4% CRP1.1 (14.8 and 59.1 mg nicotine/L PBS, indicated as low and medium, respectively [Table 2]) or 1% and 5% GCW (13.5 and 67.6 mg nicotine/L PBS, indicated as low and medium, respectively [Table 2]).

3.2. Histological assessment

The impact of exposure on tissue morphology was evaluated by histological assessment in cultures collected 4 and 24 h PE to CRP1.1 and GCW extracts or 3R4F TPM. CRP1.1 extract exposure did not cause major alterations to the culture morphology: gingival cultures, even those exposed to 738.6 mg/L concentration, resembled the PBS-exposed controls at both PE time points (Fig. 2A and Supplementary Fig. 1). GCW extract-exposed samples also resembled the PBS-exposed controls. Only following exposure to the high GCW extract concentration (811.0 mg/L), at 24 h PE, were there signs of atrophy, cell alterations, hypergranulosis, and parakeratosis (Fig. 2A).

TPM induced pronounced morphological alterations at the 50.7 mg/L concentration starting from 4 h PE (Supplementary Fig. 1), and increasing up to 24 h PE (Fig. 2A). In particular, marked atrophy, hypergranulation, and parakeratosis were observed. Cell alterations, including nuclear changes with loss of cell polarity and increased nuclear/cytoplasmic ratio, were also observed. The four-fold lower TPM concentration caused less marked changes, showing increased keratinisation, mildly increased atrophy, hypergranulosis, and parakeratosis only at 24 h PE. The score distribution for these histological findings are illustrated in Fig. 2B; for a more comprehensive view of all histological findings and their distribution, see Supplementary Fig. 2.

Controls treated with PBS and those exposed to PBS containing 2% ethanol had similar morphology, indicating that the concentration of ethanol in the TPM dilutions and the corresponding sham did not affect the epithelial structure of gingival cultures.

To investigate possible effects on cell-cell adhesion in gingival cultures exposed to CRP1.1 and GCW extracts, and TPM, we assessed the expression of E-cadherin by immunostaining. E-cadherin is a calcium-dependent adhesion molecule (van Roy and Berx, 2008) and acts as a receptor in cell junctions, with important functions in adhesion and signaling (Tsang et al., 2012; van Roy and Berx, 2008). As more pronounced morphological alterations were observed 24 h PE, we focused on this time point for our analysis of the of E-cadherin expression. Fig. 2C illustrates that there was no major alteration in E-cadherin expression at 24 h following exposures to CRP1.1 and GCW extracts at low and medium nicotine concentrations. However, there was a slight loss of apical E-cadherin expression following exposure to the high CRP1.1 and GCW extract concentrations (738.6 and 811.0 mg/L, respectively). TPM-exposed cultures showed a progressive apical decrease in E-cadherin staining at the high concentration, concomitant with the atrophy of the non-keratinized suprabasal layers.

The controls exposed to PBS and those exposed to PBS-2% ethanol did not exhibit differences in E-cadherin staining.

Table 1
Summary of chemical analyses for nicotine and TSNAs in the tobacco product preparations (100% concentrated).

Sample	Nicotine (mg/L PBS/EtOH ± SEM)	NNN (ng/mL PBS/EtOH ± SEM)	NNK (ng/mL PBS/EtOH ± SEM)	NAT (ng/mL PBS/EtOH ± SEM)	NAB (ng/mL PBS/EtOH ± SEM)
CRP1.1	1477.11 ± 26.75	29.28 ± 0.36	7.88 ± 0.08	24.09 ± 0.28	0.99 ± 0.03
GCW	1351.73 ± 63.26	40.26 ± 0.50	11.99 ± 0.11	27.61 ± 0.21	1.45 ± 0.06
TPM	2533.39 ± 130.48	459.67 ± 10.24	343.52 ± 7.12	389.80 ± 7.01	33.16 ± 0.48

Abbreviations: CRP1.1, CORESTA Reference Product 1.1; EtOH, ethanol; GCW, General Classic White; TPM, total particulate matter; NNN: N′-nitrosonornicotine; NAT: N′-nitrosoanatabine; NAB: N′-nitrosoanabasine; NNK: 4-(methylnitrosamino)-1-(3-pyridyl)-1-butanone; PBS, phosphate-buffered saline; SEM, standard error of the mean; TPM, total particulate matter. N = 9.

Table 2
Experimental groups and concentrations.

CRP1.1 group (Nicotine concentration in mg/L PBS)	GCW group (Nicotine concentration in mg/L PBS)	TPM group (Nicotine concentration in mg/L PBS)
Sham - 0% * (0)	Sham - 0% * (0)	Sham - 0% TPM (0)
Low - 1% CRP1.1 (14.8)	Low - 1% GCW (13.5)	Low - 0.5% TPM (12.7)
Medium - 4% CRP1.1 (59.1)	Medium - 5% GCW (67.6)	High - 2% TPM (50.7)
High - 50% CRP1.1 (738.6)	High - 60% GCW (811.0)	NA

The comparable concentrations of the different products are based on the nicotine concentrations (indicated in parenthesis) and displayed on the same rows. * The shams used for the snus products extracts were the same for CRP1.1 and GCW groups. Abbreviations: CRP1.1, CORESTA Reference Product 1.1; GCW, General Classic White; NA, not applicable; PBS, phosphate-buffered saline; TPM, total particulate matter. The concentrations were calculated based on the values indicated in Table 1.

3.3. Snus extract and TPM impact on the transcriptome

To comparatively quantify the biological impact of the various exposure, we employed the network-based systems toxicology approach that was used previously for the evaluation of a candidate modified risk tobacco product (MRTP) in the same and other organotypic models (Iskandar et al., 2017a, 2017b; Zanetti et al., 2016, 2017). This approach complements classical toxicological measurements by examining perturbations of the underlying molecular mechanisms based on genome-wide profiling of RNA transcripts. Additionally, the fact of including an *a priori* set collection of biological mechanisms (28 causal network models) enabled a less targeted evaluation of the relevant exposure effects, which contributes to a more objective assessment of the biological impact.

To obtain a comprehensive view of the cellular and molecular alterations induced by Swedish snus extracts and 3R4F TPM in the gingival cultures, we quantified mRNA alterations at 4 and 24 h PE. Snus exposure was associated with a maximum of 2385 and 2783 differentially expressed genes, for CRP1.1 and GCW extracts, respectively. A larger number of differentially expressed genes (maximum 6952) were instead observed following TPM exposure (Supplementary Fig. 3).

To quantitatively assess the perturbation of toxicologically relevant causal networks, we analyzed the transcriptomics data by a network-based systems toxicology impact assessment (Hoeng et al., 2014; Iskandar et al., 2017c; Martin et al., 2014). The hierarchical organization of the networks allowed for the quantitative assessment of the overall perturbation of the system by a given exposure (represented as the Relative Biological Impact Factor [RBIF]); of the perturbation of the four constituting network families (cell fate [CFA], cell proliferation [CPR], cellular stress [CST], and inflammatory process networks [IPN] (Boué et al., 2015)); and of the perturbation of each causal biological network within each network family.

Fig. 3A shows the overall biological impact, in the context of the biology covered in the network models, for each exposure condition compared with the respective sham controls (PBS for CRP1.1/GCW and PBS-2% ethanol for TPM). At the 4 h PE time point, TPM (50.7 mg/L) exposure produced the highest impact on the cultures; thus, the RBIF was set to 100% as the reference (REF). At 24 h PE, the BIF decreased, whereas the opposite trend was observed for exposure to low TPM concentration (12.7 mg/L). At low and medium concentration, the CRP1.1 and GCW extract exposure did not exert a significant biological impact, whereas at the high nicotine concentrations, a BIF value similar to that elicited by the low TPM concentration was observed. It should be noted that BIF was reduced with increasing PE time in cultures exposed to either CRP1.1 or GCW extracts. No relevant alteration was observed by the exposure with the PBS-2% ethanol (sham for TPM).

The pie charts below the BIF barplot (Fig. 3B) show the contribution of the different biological processes (network families) to the overall BIF for each exposure. The network families affected mostly by TPM exposure were CST (in yellow), CFA (in green), and IPN (in violet), compared with the PBS-2% ethanol controls.

After exposure to the low concentration of CRP1.1 and GCW extracts, the were no noticeable effects on the network families of interest (CRP1.1 [4 h PE]), in accordance with the absence of BIF, or a marginal effect concerning only one network family was observed (IPN for CRP1.1 [24 h PE], CST for GCW [4 h PE], and CFA for GCW [24 h PE]). Following exposures to the medium and high concentrations of CRP1.1 and GCW extracts, the proportional contribution of the network families composing the BIF were similar to that observed following TPM treatment, indicating a similar pattern of response to snus extracts and TPM (as indicated also by the δ values above each bar).

Each network family comprises a set of network models and can be decomposed further to network level. Fig. 3C shows the perturbation of each network (as indicated by the NPA) across the comparisons (i.e. for the different exposure conditions compared with the corresponding sham control at a given PE time point).

TPM exposure affected the majority of networks analyzed significantly. In the CFA family, the networks significantly perturbed were *Senescence*, *Necroptosis*, and *Apoptosis*; CST- and IPN-related networks were also severely perturbed by TPM exposure, independent of concentrations, with *Xenobiotic Metabolism Response* and *Oxidative Stress* primarily affected among the other networks. CPR-related networks (e.g. *Hox*, *Hedgehog*, *Cell Cycle*, *Calcium*) showed, in many cases, an exacerbation of the response with the PE time.

At the low and medium nicotine concentrations (14.8, 59.1, 13.5, and 67.6 mg/L), CRP1.1 and GCW extracts had a minimal impact, if any, for any contrast and PE time point. Following exposure to the high CRP1.1 and GCW extract concentrations (738.6 and 811.0 mg/L), the impact on the networks was instead similar to that caused by exposure to the low TPM concentration. *Xenobiotic Metabolism Response* was the only network much less affected in samples exposed to the high concentrations of snus extract compared with those exposed to the low concentration of TPM (12.7 mg/L). The possible genes/mechanisms underlying this differential perturbation are analyzed in more details in Section 3.6.

The perturbation scores following the PBS-2% ethanol treatment were comparable to those following PBS only treatment, although a few minor alterations were observed (i.e. *Senescence*, *Necroptosis*, *Apoptosis*, *Mapk*, *Jak Stat*, *Growth Factor*, *Cell Cycle*, *Oxidative Stress*, *Hypoxic Stress*, *Endoplasmic Reticulum Stress*, and *Epithelial Innate Immune Activation* networks exhibited weak perturbations, particularly at the 24 h PE time point).

3.4. Snus extract and TPM impact on miRNA expression

We complemented the network-based biological impact analyses by miRNA expression profiling and functional inferences to assess the extent to which miRNA-based transcription and regulatory programs were engaged by the different exposures. The miRNA microarray technology used in this study quantified the expression differences of 533 detected human miRNAs. CRP1.1 and GCW extracts at the high concentrations (738.6 and 811.0 mg/L, respectively) induced 139 and 122 differentially expressed miRNAs, respectively, while 3R4F TPM exposure resulted in a maximum of 236 differentially expressed miRNAs (Fig. 4A, 50.7 mg/L). Interestingly, while miRNA expression in cultures exposed to TPM was exacerbated with time, in the CRP1.1 and GCW extract-

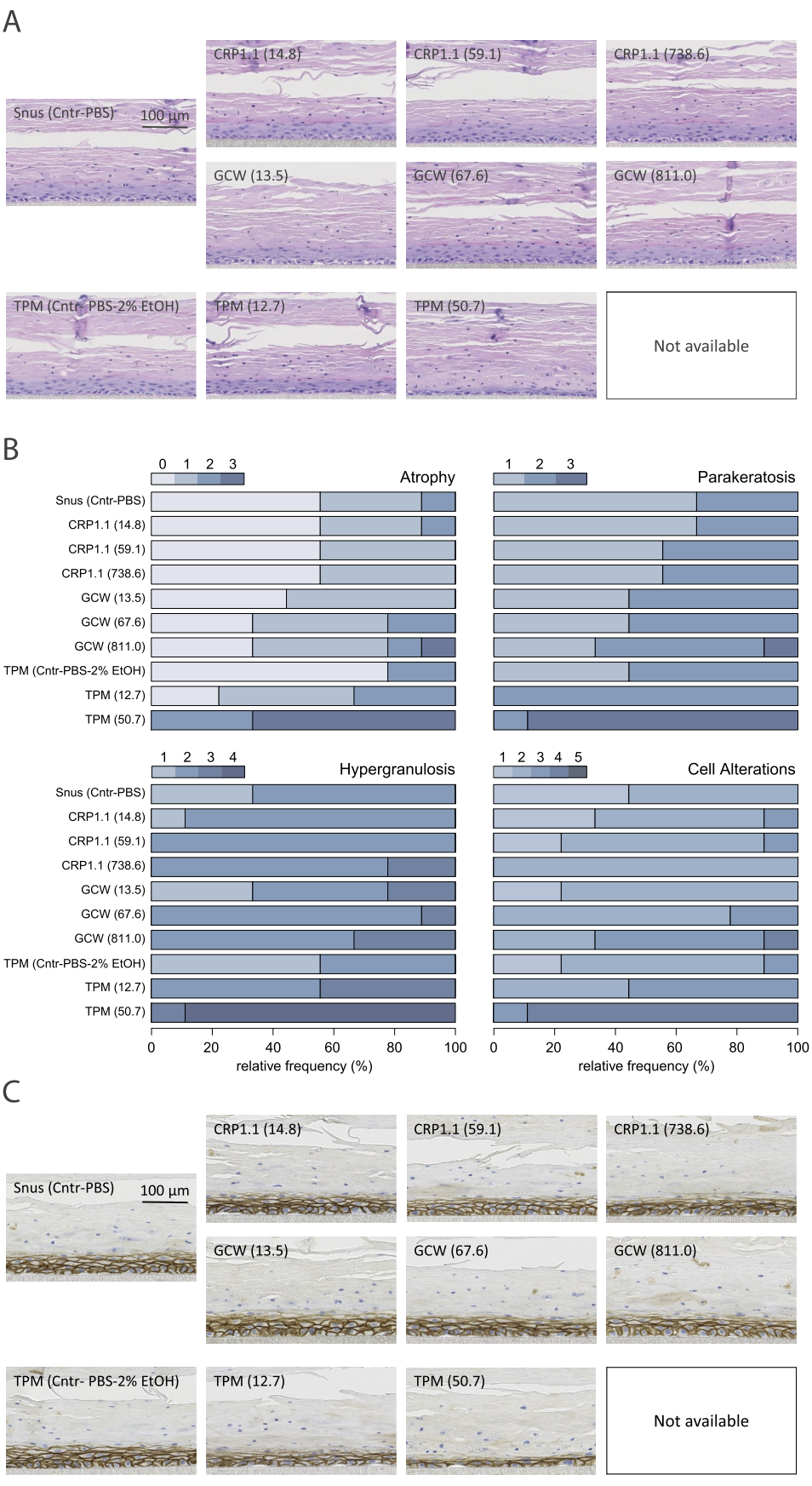

Fig. 2. Histological assessment of gingival organotypic cultures following exposure to CRP1.1, GCW extracts, and 3R4F TPM. (**A**) Representative images of H&E-stained gingival cultures 24 h following exposure to CRP1.1, GCW extracts, and TPM. Images were captured at a 40 × magnification. N = 9. (**B**) Relative frequencies of the histology scores attributed to the experimental groups 24 h following exposure to the different study treatments. Color scaling is based on the score level indicated above each finding. (**C**) E-cadherin-stained gingival cultures 24 h following exposure to CRP1.1, GCW extracts, and TPM. Images were captured at a 40 × magnification. N = 9. Concentrations are indicated in parentheses (mg nicotine/L). Abbreviations: Cntr, control; CRP1.1, CORESTA Reference Product 1.1; EtOH, ethanol; GCW, General Classic White; PBS, phosphate-buffered saline; TPM, total particulate matter.

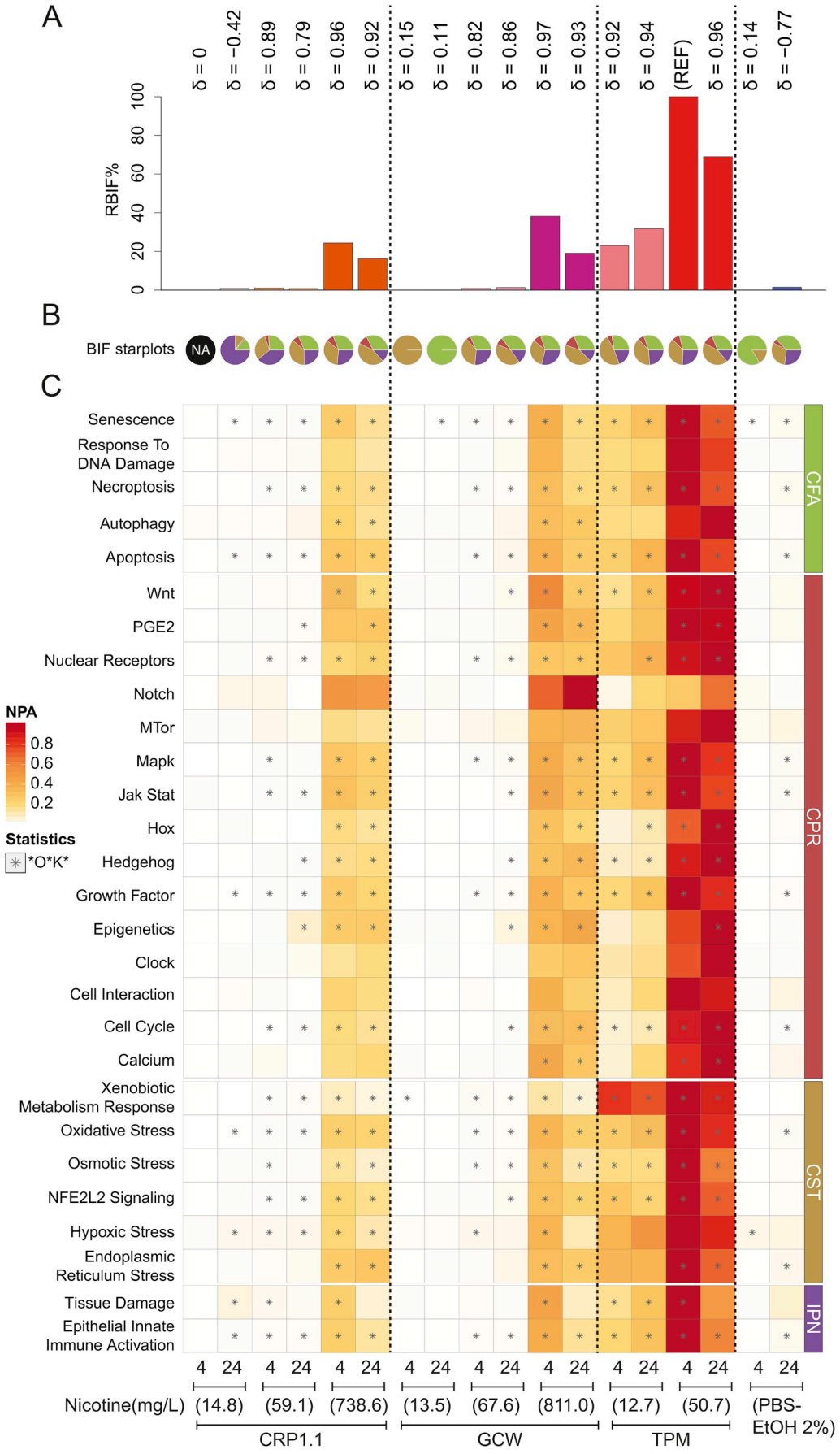

Fig. 3. Analysis of biological networks impacted by CRP1.1, GCW extracts, and 3R4F TPM exposure. (**A**) The RBIF (%) is plotted on the *y*-axis. The highest BIF is labelled as REF and was considered 100%. The δ values (δ in [−1, 1]) above the plot indicate how similar the underlying networks, which were perturbed in a particular test, were with respect to the underlying networks in the REF; δ = 0 indicates no similarity, δ = 1 indicates identical underlying network perturbations, and δ = −1 indicates completely opposite underlying network perturbations. (**B**) Each pie-chart represents the corresponding bar in the BIF plot. The charts show the decomposition of the BIF into the different network families for each comparison. One pie slice indicates one of the network families: CFA (green), CST (yellow), CPR (red), and IPN (violet). The area of the slices represents the relative contribution of each network perturbation to the BIF for a given comparison. (**C**) Heatmap of the network perturbation amplitude scores. The network names are displayed on the left side of the heatmap, with the corresponding network family names on the right. The shading gradient of the NPA score was normalized to the highest NPA score per network. A network was considered significantly perturbed if the NPA score was significant for all three associated statistics (i.e. the 95% uncertainty interval of the biological variability does not contain the zero value, and the "*O"/"K*" network specificity statistics have a *p*-value smaller than 0.05). O and K statistics indicate the specificity of the NPA score with respect to the biology represented by each network. Concentrations are indicated in parentheses (mg nicotine/L). Times represented (4, 24) refer to hours PE. Abbreviations: BIF, Biological Impact Factor; CFA, cell fate; CST, cell stress; CPR, cell proliferation; EtOH, ethanol; IPN, inflammatory process network; PBS, phosphate-buffered saline; NA, not available; NPA, network perturbation amplitude; REF, reference; RBIF, relative BIF. N = 8–9.

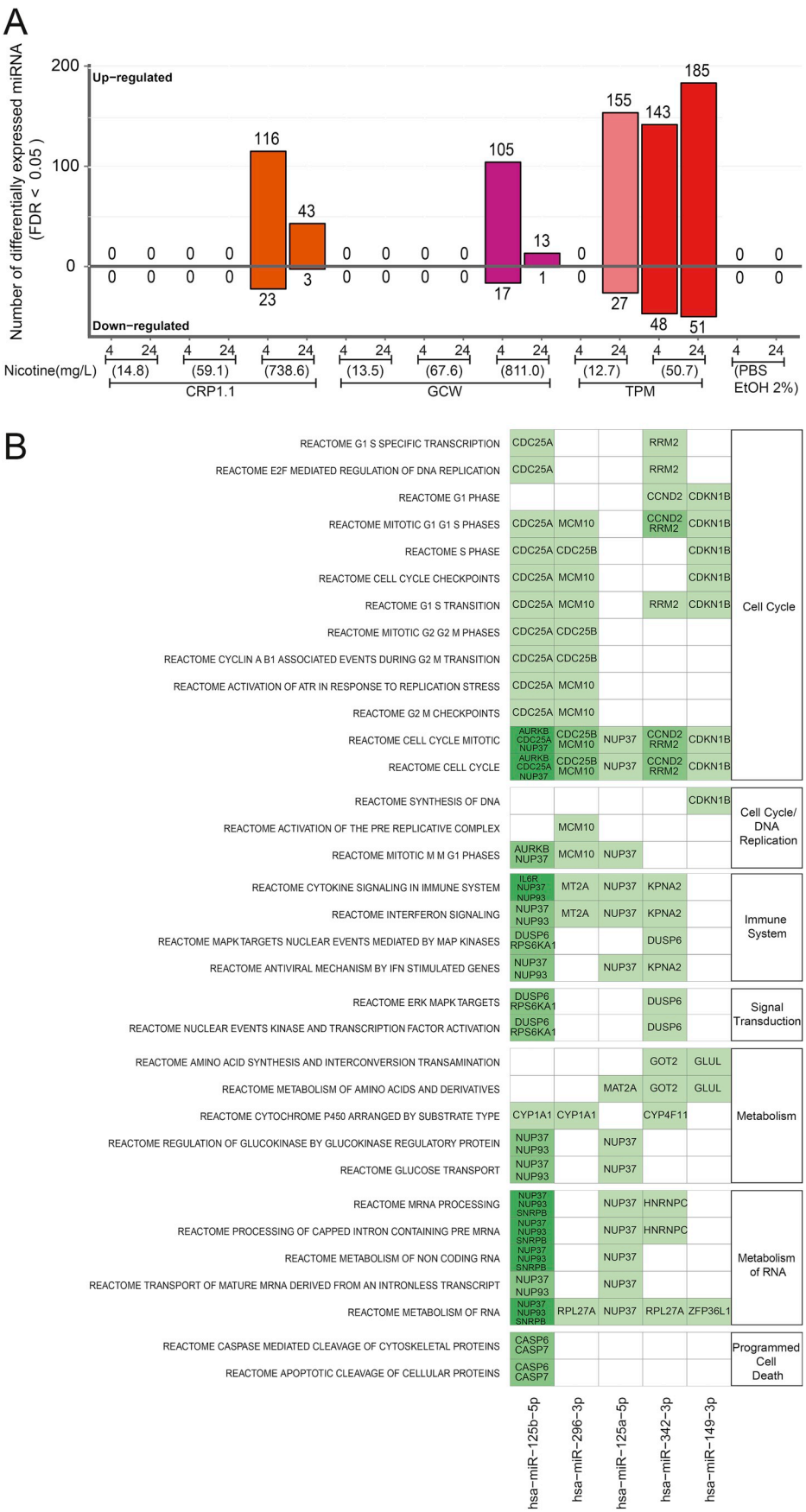

Fig. 4. Results of the inference of relevant miRNAs with biological functions. (**A**) Numbers of differentially expressed miRNAs in exposed cultures relative to sham-exposed controls. Each bar displays the numbers of miRNAs significantly altered for each exposure condition indicated in the *x*-axis (the positive values correspond to increased expression and the negative values to decreased expression compared with the sham-exposed controls). Times represented (4, 24) refer to hours PE. Concentrations are indicated in parentheses (mg nicotine/L). (**B**) Heatmap displaying the miRNA-target mRNA-pathway associations obtained from the integrated computational pipeline (see the Materials and Methods). To select the most reliable associations, we restricted the results from (**A**) to the high-confidence miRNAs defined by miRBase (Kozomara and Griffiths-Jones, 2014), which are more likely to effectively exert a biological function. The mRNAs expected to be regulated by a given miRNA for a given pathway are represented in the cell intersecting the respective pathway row and the miRNA column. Supplementary Fig. 4 contains the complete version of this heatmap, which includes a few additional miRNAs and pathways that were removed for insufficient support and non-relevant biology, respectively. Abbreviations: FDR, false discovery rate; CRP1.1, CORESTA Reference Product 1.1; EtOH, ethanol; GCW, General Classic White; PBS, phosphate-buffered saline; TPM, total particulate matter. N = 8–9.

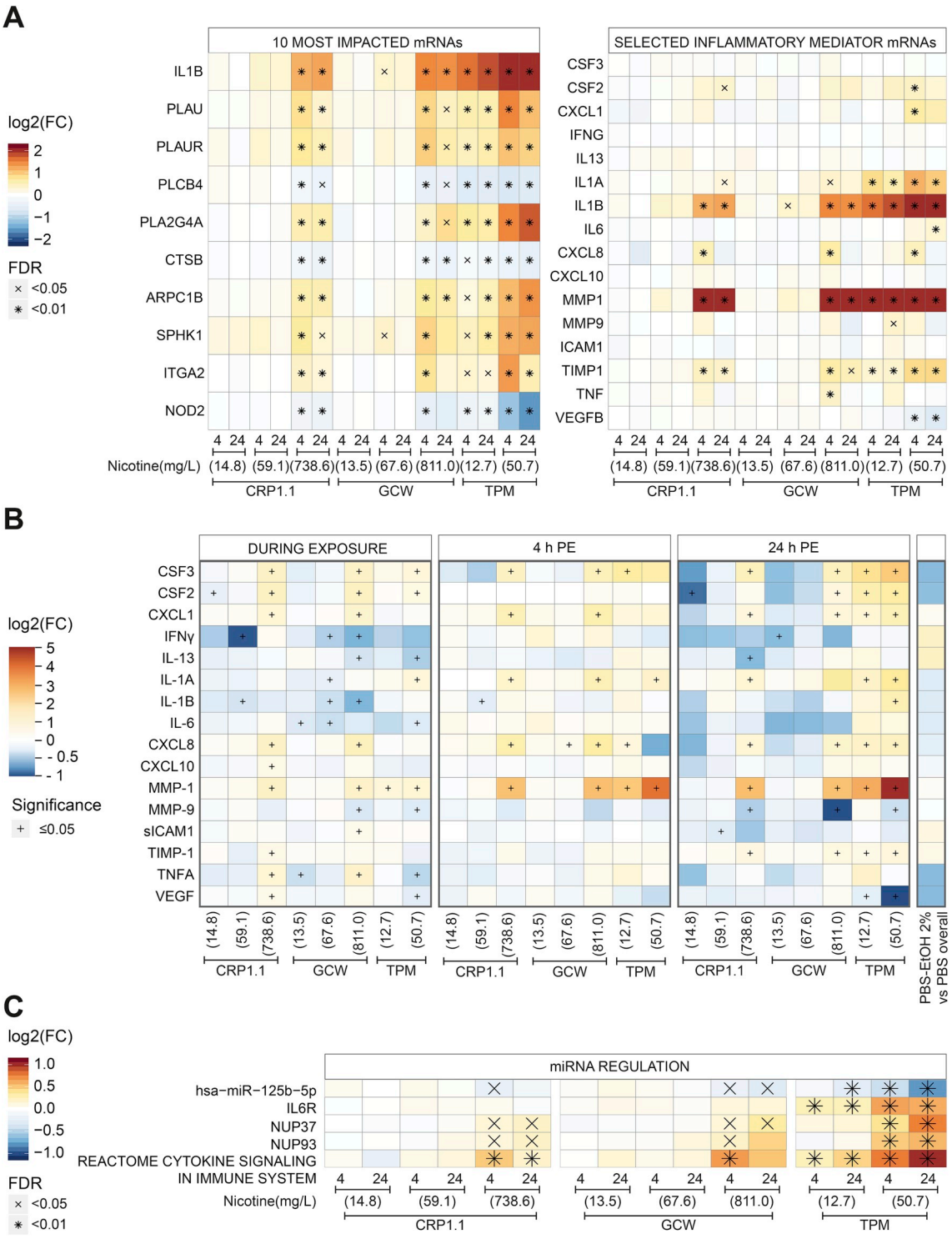

Fig. 5. Inflammatory response upon exposure to CRP1.1, GCW extracts, and 3R4F TPM. (**A**) The heatmap on the left shows the differential expression of the 10 most altered genes related to inflammation in gingival cultures; the heatmap on the right shows the differential expression of selected inflammatory genes. ^{x} and * indicate statistically significant differential expression (FDR < 0.05 or FDR < 0.01, respectively), as explained in the Materials and Methods. Times represented (4, 24) refer to hours PE. Concentrations are indicated in parentheses (mg nicotine/L). N = 8–9. (**B**) Heatmap showing the fold changes of mean concentrations of secreted inflammatory mediators in the basolateral media at the completion of the 72-hour exposure to TPM, CRP1.1, and GCW extracts "During Exposure", and 4 and 24 h PE, relative to the concentrations of the corresponding sham controls. Concentrations are indicated for each group (mg nicotine/L, *x*-axis). $^{+}$ indicates statistically significant differential expression ($p \leq 0.05$), as explained in the Materials and Methods. N = 9. (**C**) Heatmap displaying the characteristic exposure responses of an inflammation-associated high-confidence miRNA, miR-125b-5p, its inferred target mRNAs (IL6R, NUP37, and NUP93), and the pathway *Cytokine Signaling in Immune System* (cluster "Immune System" in Fig. 4B). For miRNAs and mRNAs, the exposure response corresponds to the differential expression values and their associated FDR, whereas for pathways, the row normalized scores are shown, accompanied by their Q2 FDR (Materials and Methods). Times represented (4, 24) refer to hours PE. Concentrations are indicated in parentheses (mg nicotine/L). N = 8-9. Abbreviations: FDR, false discovery rate; CRP1.1, CORESTA Reference Product 1.1; EtOH, ethanol; GCW, General Classic White; PBS, phosphate-buffered saline; PE, post-exposure; TPM, total particulate matter.

exposed cultures, the number of impacted miRNA was reduced to 46 and 14, respectively, at 24 h PE.

Similarly to our previous study (Zanetti et al., 2018), we applied an integrated computational analysis to identify candidate biological functions regulated by miRNAs and categorized the implicated miRNAs according to their specific association with pathway categories (see Materials and Methods). These results revealed 10 high-confidence responding miRNAs that could collectively downregulate up to 143 target mRNAs corresponding to 57 significantly enriched Reactome pathways grouped in 11 high-level categories (Fig. 4B, which displays selected miRNA-mRNA-pathway extracted associations relevant for the biological context; for the complete list, see Supplementary Fig. 4). The affected pathway categories included processes relevant to oral disease pathology, such as Cytokine Signaling, Cytochrome P450, and processes related to the cell cycle. Often, multiple pathways were associated with the same miRNAs: this reflects the fact that the intermediate target mRNAs were included in multiple pathways and that a closer examination of the biological context is necessary to determine which ones are the most relevant.

Given the inferred associations between relevant subsets of miRNAs,

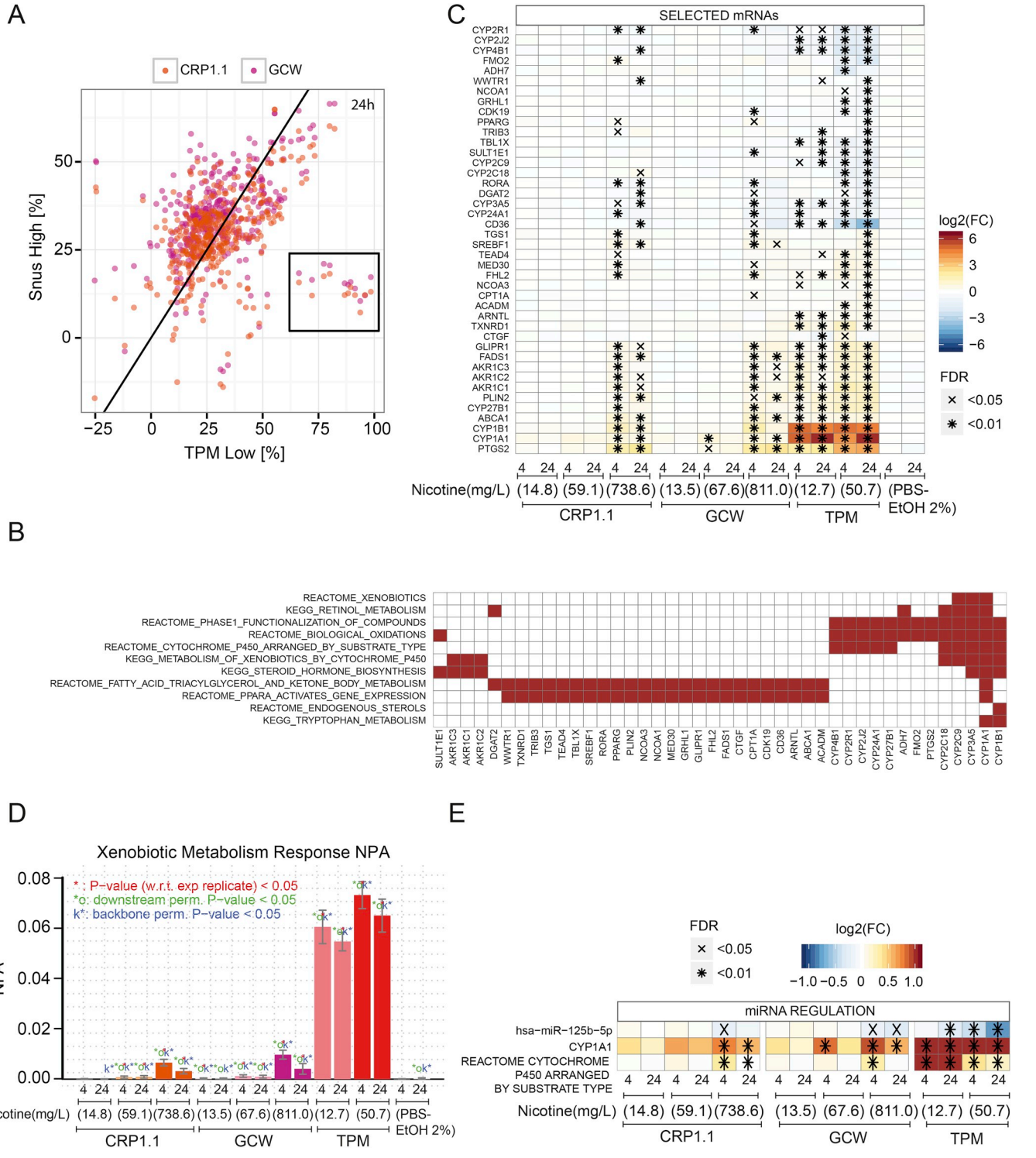

(caption on next page)

Fig. 6. Differential regulation of mRNA/miRNA involved in xenobiotic metabolism processed by CRP1.1, GCW extracts, and 3R4F TPM exposures. (**A**) The gene set response comparison identified a group of gene sets that is, relative to that perturbed by exposure to TPM at the high concentration, less perturbed by exposure to TPM at low concentrations or to CRP1.1 and GCW extracts at high concentrations at 24 h PE. Each point represents the relative gene set effect for low-concentration TPM (*x*-axis) and high-concentration snus extracts (*y*-axis) for a gene set from the c2. cp collection (Liberzon et al., 2011) at 24 h PE. Gene set effects are estimated as the group-averaged first principal component score of the gene set. The group of candidate outlying gene sets is marked with a black box. (**B**) Identified gene sets less activated by exposure to CRP1.1 and GCW extracts at high concentrations than by exposure to TPM at low concentrations at 24 h PE. On the *y*-axis, the gene sets are reported; the *x*-axis reports genes dominantly contributing to the gene set scores (leading genes marked by red cells) that were identified for at least two of these gene sets. (**C**) Identified mRNA (reported in (**B**)) from gene sets less activated by exposure to CRP1.1 and GCW extracts at high concentrations than by exposure to TPM at low concentrations at 24 h PE. ^{X} and * indicate statistically significantly differential expression of mRNA and miRNA (FDR $<$ 0.05 or FDR $<$ 0.01, respectively), as explained in the Materials and Methods. (**D**) Network perturbation amplitude (NPA) scores for the *Xenobiotic Metabolism Response* network. The *Xenobiotic Metabolism* network was considered significantly perturbed if the NPA score was significant for all three associated statistics (i.e. the 95% uncertainty interval of the biological variability does not contain the zero value, and the "*O"/"K*" network specificity statistics have a p-value smaller than 0.05). O and K statistics indicate the specificity of the NPA score with respect to the biology represented by each network. (**E**) Heatmap displaying the exposure responses of the xenobiotic metabolism-specific ("*Reactome Cytochrome P450 Arranged by Substrate Type*" in Fig. 4B) high-confidence miRNA, miR-125b-5p, and its inferred target mRNAs and associated pathways. For miRNAs and mRNAs, the exposure response corresponds to differential expression values and associated FDR, whereas for the pathways the mean score is shown, accompanied by the overrepresentation FDR (shown in Fig. 4B). ^{X} and * indicate statistically significantly differential expression (FDR $<$ 0.05 or FDR $<$ 0.01, respectively), as explained in the Materials and Methods. Concentrations are indicated for each group (mg nicotine/L, x-axis). Times represented (4, 24) refer to hours PE. Abbreviations: FC, fold change; FDR, false discovery rate; CRP1.1, CORESTA Reference Product 1.1; EtOH, ethanol; GCW, General Classic White; NPA, network perturbation amplitude; PBS, phosphate-buffered saline; PE, post-exposure; TPM, total particulate matter. N = 8–9.

target mRNA, and pathways, we returned to the overall study purpose of biological impact assessment and examined how these coordinated molecular responses were differentially activated following exposure to CRP1.1, GCW extracts, and TPM. Clearly, the strongest effects resulted from exposure to TPM (Supplementary Fig. 5). These are explained in more detail in the following paragraphs, where we analyzed in greater depth the contributions of selected high-confidence triplets (miRNA, target mRNA, pathways) to different biological processes involved in oral health and tobacco product response.

3.5. Snus extract and TPM exposure-induced inflammatory response

Inflammation is a pivotal process in the context of periodontal diseases (Giannopoulou et al., 2003; Guentsch et al., 2008) with cigarette smoking being a known risk factor. So far, we have established that the impact of Swedish snus exposure and 3R4F TPM on the IPN differed and implicated miRNAs in the regulation of the inflammatory response.

In this section, we investigate the effect of Swedish snus and TPM on the inflammatory response in more detail. For this, we complemented inflammation-related gene/miRNA expression profiling with profiles of inflammatory mediators in the basolateral media collected during exposure (three aliquots pooled together, see the Materials and Methods) and at 4 and 24 h PE.

The heatmap in Fig. 5A (left panel) illustrates the 10 most altered inflammation-related genes (by FC) in gingival organotypic cultures following exposure to CRP1.1 and GCW extracts, or TPM (see Supplementary Fig. 6 for a larger gene set). *IL1B* was the most upregulated inflammatory gene, significantly higher than controls, particularly following exposure to CRP1.1 and GCW extracts at the high concentrations (738.6 and 811.0 mg/L), and to TPM at both concentrations (12.7 and 50.7 mg/L). *PLAU*, *PLAUR*, *PLA2G4A*, *ARPC1B*, *SPHK1*, and *ITGA2* were also among the most upregulated genes, following the same pattern described for *IL1B*. *PLCB4*, *CTSB*, and *NOD2* were instead downregulated by exposure to the high concentrations of CRP1.1 and GCW extracts and TPM (12.7 and 50.7 mg/L).

To further evaluate the inflammatory response, we selected a panel of inflammatory mediators that are important in the context of oral diseases (Barros et al., 2016; Isaza-Guzmán et al., 2015; Rathnayake et al., 2013) and examined their gene expression (Fig. 5A, right panel) as well as protein secretion in the basolateral medium (Fig. 5B). MMP-1 was the inflammatory mediator most upregulated by exposure to the high CRP1.1 and GCW extract concentrations and TPM and at both the gene expression and protein secretion levels. IL-1B secretion exhibited a different trend compared with its gene expression, increasing only following TPM exposure (50.7 mg/L, 24 h PE), whereas it decreased during exposure to CRP1.1 (59.1 mg/L) and GCW (67.6 and 811.0 mg/L) extracts. IL-1A was mainly increased by TPM exposure (12.7 and 50.7 mg/L) at both the gene expression and protein secretion levels. TIMP-1 gene expression (4 and 24 h PE) and protein secretion (24 h PE) were instead increased by exposure to CRP1.1 and GCW extracts (738.6 and 811.0 mg/L, respectively) and TPM (12.7 and 50.7 mg/L).

In summary, at the low and medium concentrations, CRP1.1 and GCW extracts exerted a limited effect on the secretion of inflammatory mediators, whose medium levels remained close to control levels, significantly affecting the secretion of only few analytes during exposure (e.g. IFNγ by CRP1.1 [59.1 mg/L]) and PEs (e.g. CSF2 by CRP1.1 [14.8]). In contrast, the high concentrations elicited a more marked effect, with significant alteration in the secretion of several mediators. In general, the impact of CRP1.1 and GCW extracts on the secretion of inflammatory mediators tended to decrease or remain stable with PE time, whereas the effects of TPM further increased over time. No mediator was significantly altered in PBS-2% ethanol controls compared with PBS controls.

To better compare the inflammatory response, we also directly contrasted the FC response of the secreted mediators (Supplementary Fig. 7): CRP1.1 and GCW extract showed a comparable response and TPM induced a stronger response than snus extracts, particularly for CSF2/3, CXCL1, IL-1A, IL-8, MMP-1, TNFA, and VEGF.

Finally, one of the identified high-confidence miRNAs (Fig. 4B), miR-125b-5p, was inferred to be involved in regulation of the inflammatory response by modulating the *Cytokine Signaling in Immune System* pathway, with *IL6R*, *NUP37*, and *NUP93* as its predicted target genes (Fig. 5C). The levels of miR-125b-5p negatively correlated with an increased expression of *NUP37* and *NUP93*, but not *IL6R*, upon exposure to the high CRP1.1 and GCW extract concentrations (738.6 and 811.0 mg/L); notably, *NUP37* and *NUP93* were not upregulated by the low TPM concentration (12.7 mg/L), while *IL6R* was affected by both TPM concentrations. These results may indicate a threshold effect in the regulation of target genes by miR-125b-5p.

3.6. Xenobiotic metabolism activation by snus extract and TPM

When testing the high snus extract concentrations, both CRP1.1 and GCW extracts induced a clear molecular response that reached (e.g. with respect to the BIF) the amplitude of the response observed for the low TPM concentration. Notably, this effect was induced at an at least 58-fold higher nicotine concentration for snus extracts (738.6 mg/L for CRP1.1, 811.0 mg/L for GCW) than for TPM (12.7 mg/L). At these concentrations, the engaged biological processes following CRP1.1 and GCW extracts and TPM exposure appeared generally similar (Fig. 3C), indicating activation of a generic exposure response involving a broad range of biological processes.

As a follow up, we investigated whether any biological process would be more distinctly associated with snus extract or TPM exposure at these exposure concentrations with overall similar amplitudes of the biological responses. We compared the 24 h PE impact of the high CRP1.1 and GCW extract concentrations (738.6 and 811.0 mg/L) with that of the low TPM concentration (12.7 mg/L) on the dominant directions of change for a large gene set collection (c2. cp collection from MSigDB (Liberzon et al., 2011)) (Fig. 6A). While the majority of evaluated gene sets demonstrated a similar response following exposure to the snus extract and TPM at these concentrations, a small subset showed a substantially lower engagement following snus extract (< 25% of high TPM) than following low TPM (> 60% of high TPM) exposure (Fig. 6A, black rectangle).

Interestingly, these outlying gene sets were dominantly associated with the xenobiotic metabolism response (Fig. 6B), prominently including *CYP1A1* and *CYP1B1*. Confirming this observation for the 24-hours PE time point, 10 of these 11 gene sets were also identified as an outlying group for the 4-hours PE time point (Supplementary Figs. 8A and B). Furthermore, lower engagement of xenobiotic metabolism gene sets following exposure to high snus extract concentrations than following low concentration TPM exposure was also supported by an alternative gene set scoring approach (Supplementary Figs. 8C and D) and by the causal network enrichment approach: although the majority of evaluated biological networks was similarly perturbed following these exposures, the *Xenobiotic Metabolism Response* network showed a much lower (relative) activation by snus than by TPM (Figs. 3C and 6D). This finding confirms the lower engagement of xenobiotic metabolism-related processes in cultures following exposure to snus extracts (high concentration) that were different from the activation of xenobiotic metabolism response following TPM treatment.

Among the xenobiotic genes driving these differences, *CYP1A1* and *CYP1B1* showed the most pronounced differences following the exposure conditions, with the highest FCs (versus sham) among all contributing genes (Fig. 6C).

Among the high-confidence miRNAs represented in Fig. 4B, miR-125b-5p was inferred to be involved in the regulation of the cytochrome P450 signaling pathway and the target gene *CYP1A1* (Fig. 6E). The downregulation of this miRNA was observed mainly in gingival cultures exposed to TPM, proportional to the concentration and PE time. CRP1.1 and GCW extracts slightly downregulated miR-125b-5p at high concentrations (738.6 and 811.0 mg/L).

Taken together, the results presented in this section support a clear mechanistic difference in the exposure response, with a much lower engagement of xenobiotic metabolism processes (particularly, *CYP1A1* and *CYP1B1* activation) by CRP1.1 and GCW extracts than by TPM exposure.

4. Discussion

Swedish snus is considered a less harmful alternative to tobacco smoking, as 1) the tobacco is not burned, thus reducing the formation of HPHCs (Asplund et al., 2003); 2) this product is manufactured with a procedure that minimizes the level of toxicant compounds (Rutqvist et al., 2011); 3) epidemiological studies conducted since the 1970s have indicated no association of snus with oral and pancreatic cancers (Bertuccio et al., 2011; Lewin et al., 1998); and 4) a recent study by Ramström and colleagues (Ramstrom et al., 2016) indicates that switching to snus can help accomplish smoking cessation.

In vitro studies investigating the impact of snus thus far often lacked the use of cellular models resembling the human situation, as, for example, organotypic culture models do. In addition, exposures to snus were frequently performed in the lower range of the nicotine concentration measured in the saliva of snus users, and the exposure usually was not administered for longer than 24 h.

The current study analyzed the effects of a 72-hour continuous exposure to Swedish snus extracts and those induced by TPM on human gingival epithelial organotypic cultures. We compared the effects of extracts from a commercial snus, GCW, to those of the extract from CRP1.1; TPM from cigarette smoke was used as a positive control indicative of the biological impact of a combusted tobacco fraction, although we acknowledge that TPM does not fully represent whole cigarette smoke exposure. Gingival epithelial organotypic cultures were used as *in vitro* model, as they better resemble the structure and the response to toxicants of the native gingival epithelium compared with 2D models. To our knowledge, this is the first study to assess the impact of Swedish snus on fully differentiated gingival organotypic cultures.

To be as close as possible to the human situation, we developed a protocol for snus extraction that resembles the characteristics of snus use in the oral cavity of snus consumers. Temperature and time of extraction were tested to ensure sufficient yields of nicotine and TSNAs (measured under different conditions in a previous experiment, data not shown) and to be in the range of those found in the saliva of moist snuff users: 73–1560 mg/L nicotine, maximum 16 μg/L NNK, 3–140 μg/L NNN, and 4–85 μg/L NAT (Hoffmann and Adams, 1981). The temperature and duration of extraction were also comparable with what is observed for snus users (i.e. at 37 °C [mouth temperature] for around 1 h (Digard et al., 2009)). Our results show that the nicotine and TSNA concentrations among the different preparations were reproducible over multiple experimental repetitions. PBS was selected as snus solvent because it retains a similar composition to artificial saliva but does not include biological additives that can be responsible of adverse outcomes in cell cultures (Moharamzadeh et al., 2009; Malpass et al., 2013). We also observed adverse effects on gingival cell cultures by applying apically an artificial saliva preparation (Zanetti et al., 2018). Moreover, the selection of an artificial saliva that is closely resembling the real saliva may be challenging due to the many different types of compositions available, of which some do not meet the biophysical properties of real saliva (Kho, 2014; Preetha and Banerjee, 2005).

The cultures were exposed to a high concentration of snus extracts that was in the range of the nicotine and TSNA concentrations measured in the saliva of moist snuff dippers (Hoffmann and Adams, 1981) and two concentrations matched by nicotine level with TPM. A study more recently conducted by British American Tobacco considered the salivary nicotine concentration in Swedish snus users specifically. The authors reported that a 1-h use would transfer 3.44 mg nicotine from a snus pouch (Gale et al., 2011). Considering that the average amount of saliva produced in 1 h is around 20–30 mL (Puy, 2006), the theoretical concentration of nicotine in saliva would be around 115–172 mg/L (assuming balanced mixing of saliva), which is in the lower range of what was described by Hoffmann and Adams for moist snuff users (Hoffmann and Adams, 1981). However, considering that the snus pouch placed below the upper lip is not close to the salivary glands and hence less exposed to saliva (Rutqvist et al., 2011), it can be assumed that the concentration of nicotine in the proximity of the pouch will be higher and more similar to the high snus extract concentrations used in our study.

The high nicotine concentration of TPM used in this study was about 12 times higher than the maximum measured in the saliva of smokers (Robson et al., 2010), or three times higher than the medium-inhaling smokers' salivary nicotine range from an older study (Feyerabend et al., 1982).

While the snus extract was prepared to closely mimic the human situation, TPM only represents the particulate fraction of the whole smoke, and requires an organic solvent (ethanol in our case) for efficient dissolution of the captured smoke components. Therefore, the direct comparison of the effects of these tobacco products brings some challenges. While TPM represents the constituents of the particulate phase of the smoke aerosol (including the nicotine), the hydrophilic constituents from the gas-vapor phase (including most carbonyls) can be trapped in aqueous solvents (for *in vitro* testing). However, since in the mainstream smoke nicotine mostly distributes to the particulate phase (Seeman et al., 2004), such a gas-vapor phase extract contains

only a minimal amount of nicotine, and the other nonvolatile TPM constituents, such as TSNAs, would also be underrepresented (Gao et al., 2013; Kogel et al., 2015). TPM extracted with organic solvents has the advantage of being stable and represents a known standard cigarette smoke fraction used in many *in-vitro* assays used in various regulatory guidelines (CORESTA, 2004; Crooks et al., 2013) and, thus, allows comparisons with previously published studies (Gao et al., 2013; Malpass et al., 2014; Woo et al., 2017). Guided by these considerations, we selected TPM extracted with ethanol as a positive control and representative cigarette smoke fraction in the current study that would allow the normalization to a similar nicotine concentration used for the snus products. In this context it also important to note that, while the TPM extracts contained a residual amount of 2% (v/v) ethanol from the extraction, its presence was found not to influence the response of the cultures significantly.

The biological effects elicited by exposure to snus were assessed by a systems toxicology approach. This is the first time this approach has been applied in the context of snus research. Systems toxicology provides a mechanistic understanding of the processes underlying toxicity by complementing classical systems biology with computational analyses. The resulting integrated data analysis indicates how biological pathways are perturbed by the exposure (Sauer et al., 2016; Sturla et al., 2014). Systems toxicology has the potential to reduce animal testing by combining *in vitro* testing on human-relevant models and computational methods within the framework described by the 21st Century Toxicology paradigm (Andersen and Krewski, 2009; NRC, 2007).

In humans, the effects of prolonged exposure to snus have been well studied for many years, describing increased epithelial thickness and keratinisation (Merne et al., 2002; Wedenberg et al., 1996) and rare dysplastic changes, which are normally resolved after snus cessation (Roosaar et al., 2006; Wood et al., 1994). Our results show that CRP1.1 and GCW extracts induced a minimal impact on culture morphology and E-cadherin expression at relevant concentrations for human exposure. These results differ from previous studies using 3D oral models, observing loss of cellular adhesion and severe morphological changes following 2 (Wang et al., 2001) and 12 (Merne et al., 2004) days of exposure. Of note, the study by Wang et al. employed 3D cultures of human foreskin keratinocytes, while the Merne et al. study employed immortalized skin keratinocytes, which may not resemble the characteristics and response to injury of human oral keratinocytes (Turabelidze et al., 2014). Moreover, in Merne et al. the 3D cultures were exposed at the beginning of the stratification phase, a setting that resembles a wound-healing situation rather than exposure of a mature tissue, as would be the case in the oral cavity of snus users. The effects of TPM on culture morphology illustrated in this study were instead very marked, independent from its nicotine concentration which was at least 14 times lower than that of the high snus extracts. These effects on gingival organotypic cultures resemble those that we previously showed for the exposure to whole cigarette smoke (Zanetti et al., 2017, 2018).

Inflammation is one of the main processes contributing to cigarette smoke-induced oral tissue damage. Epithelial cells participate in tissue innate immunity and respond to cigarette smoke exposure by inducing the expression of several inflammatory mediators (Johannsen et al., 2014; Lee et al., 2012; Semlali et al., 2012). Accordingly, we measured a progressive inflammatory response at the level of gene expression and – on the protein level - secretion of inflammatory mediators in TPM-exposed samples. Following exposure to snus extract, the inflammatory responses and gene expression changes were proportional to the exposure concentration. For example, we detected increased MMP-1 gene expression and protein secretion at different levels in snus and TPM-exposed cultures. The main role of MMPs is in matrix degradation and proteolytic activation of inactive inflammatory mediators (Popat et al., 2014; Sapna et al., 2014), and MMP-1 was found to be increased in oral inflammation models (Kim et al., 2006); different MMPs were activated by cigarette smoke in gingival tissues (Ozcaka et al., 2011) and in organotypic buccal and gingival epithelial cultures *in vitro* (Schlage et al., 2014; Zanetti et al., 2016, 2017, 2018). MMP-9 was downregulated by the high concentration of snus extracts and by TPM, concomitantly with an upregulation of MMPs inhibitor TIMP-1. This effect was observed previously in gingival cultures following cigarette smoke exposure (Zanetti et al., 2017).

To further complement the transcriptomics results, we investigated a possible modulation of gene expression by miRNA. To our knowledge, this is the first time that miRNAs have been investigated in relation to the effect of an STP. MicroRNA-125b-5p was predicted to modulate the expression of *IL6R*, *NUP37*, and *NUP93*, all of which are involved in cytokine signaling. The interrelationship between miR-125b-5p and *IL6R* was already described by Morelli et al. to affect growth and survival in the context of multiple myeloma (Morelli et al., 2015); *IL6R* was also a validated target of miR-125b-5p in liver cancer cells, where the pair promoted apoptosis (Gong et al., 2013). Interestingly, *IL6R* expression was not modulated by snus extracts but only by TPM; accordingly, the modulation of miR-125b-5p was higher in TPM-exposed samples than in those exposed to snus extracts.

Our network-based approach entailed in the Systems Toxicology analysis identifies processes rather than single molecules and their characterization using reverse causal reasoning goes beyond the singular measurement of transcripts in the context of biological networks (Boué et al., 2015; Catlett et al., 2013). The network nodes are not assigned mRNA differential expression values but activity “perturbation amplitudes”, which are inferred from the transcriptional effects of the genes causally affected by the changes of the activity of the network node (see Materials and Methods). This approach evidenced that, among the different networks analyzed, *Xenobiotic Metabolism Response* was the only network that exhibited markedly lower NPA scores for the cultures exposed to high-concentration snus extract than those exposed to TPM at the low concentration. Nonetheless, xenobiotic metabolism was the most perturbed process by TPM. A deeper investigation at the gene expression level revealed that this effect was driven by a group of genes that exhibited a differential response to the two different stimuli. Among those, *CYP1A1* and *CYP1B1* were the most altered by both TPM concentrations, while they were minimally affected by snus extracts. Polycyclic aromatic hydrocarbons and other often carcinogenic constituents, such as aldehydes and aromatic amines, are highly represented in tobacco smoke, but not in STP preparations due to the absence of combustion (Borgerding et al., 2012; Stepanov et al., 2010); it is possible that the differential activation of the xenobiotic metabolism-related genes is attributed to the reduction/absence of these toxicants in the snus extracts. This effect may also have been caused, at least in part, by the downregulation of miR-125b-5p, which was predicted to inhibit *CYP1A1 in silico* (Gill et al., 2017) and was observed in the human liver (Burgess et al., 2015). This finding is further strengthened by our recent report of the same correlation in buccal and gingival cultures exposed to 3R4F cigarette smoke or to an aerosol from another potential MRTP (Zanetti et al., 2018). MicroRNA-125b-5p was also downregulated at later PE time points by cigarette smoke in the buccal, nasal, and bronchial organotypic cultures tested previously (Iskandar et al., 2017c). These findings indicate a common mechanism for the regulation of miR-125b-5p among different organotypic cultures representing target tissues exposed to tobacco products, in support of the “field of injury” concept (Steiling et al., 2008).

The study by Woo and colleagues also highlighted a higher impact on the xenobiotic metabolism process by combustible tobacco product fractions (i.e. TPM and whole smoke [WS] extracts) vs. a smokeless tobacco extract ([STE], an American-type reference moist snuff) at the gene expression level in submerged gingival cell cultures (Woo et al., 2017). The study described a strong upregulation of *CYP1A1* and *CYP1B1* genes by smoke fractions but much lower by the American snuff extract. The study indicated *AKR1C1* as a potential biomarker for differentiating the biological effects of combustible and noncombustible

products; in our study, *AKR1C1* was slightly upregulated by Swedish snus extracts (Supplementary Fig. 9). Although the design of the Woo et al. study was different compared with ours concerning the nicotine concentrations of snus extracts (474 mg/L maximum), exposure duration (24 h), and culturing conditions (2D monolayer gingival cells), some other characteristics were generally comparable (i.e. use of TPM and STP, gingival cultures, and assessment of subtoxic and toxic concentrations); hence, we performed a comparative analysis integrating their transcriptomics data with our network-based systems toxicology approach. The results shown in Fig. 7 evidence several instructive findings: 1) our network-based approach for the quantification of biological impact is the most sensitive to assess the effect of these products, as both differential gene expression and GSA could not otherwise detect the TPM effects in the Woo et al. dataset; 2) subtoxic/toxic concentrations of Swedish snus and the STE yield similar RBIF values, although the nature of the perturbations they cause (i.e. the statistical significance of the perturbations of the underlying networks) are slightly different according to the δ values, as may be expected by products with a different composition; 3) the pure nicotine effect is smaller than the corresponding dose-matched STE effect; 4) TPM and WS, within the Woo et al. dataset, exert a similar impact profile (RBIF) as indicated by the δ values (0.93 vs. 100 for TPM and WS, respectively); and 5) the xenobiotic metabolism response is weaker in Swedish snus extract-exposed cultures than those exposed to the American type moist snuff, even at a higher nicotine concentration. This suggests that the xenobiotic metabolism response may not be driven by nicotine within the experimental conditions tested, though the findings would be consistent with the lower nitrosamine concentrations in Swedish snus compared with American snuff.

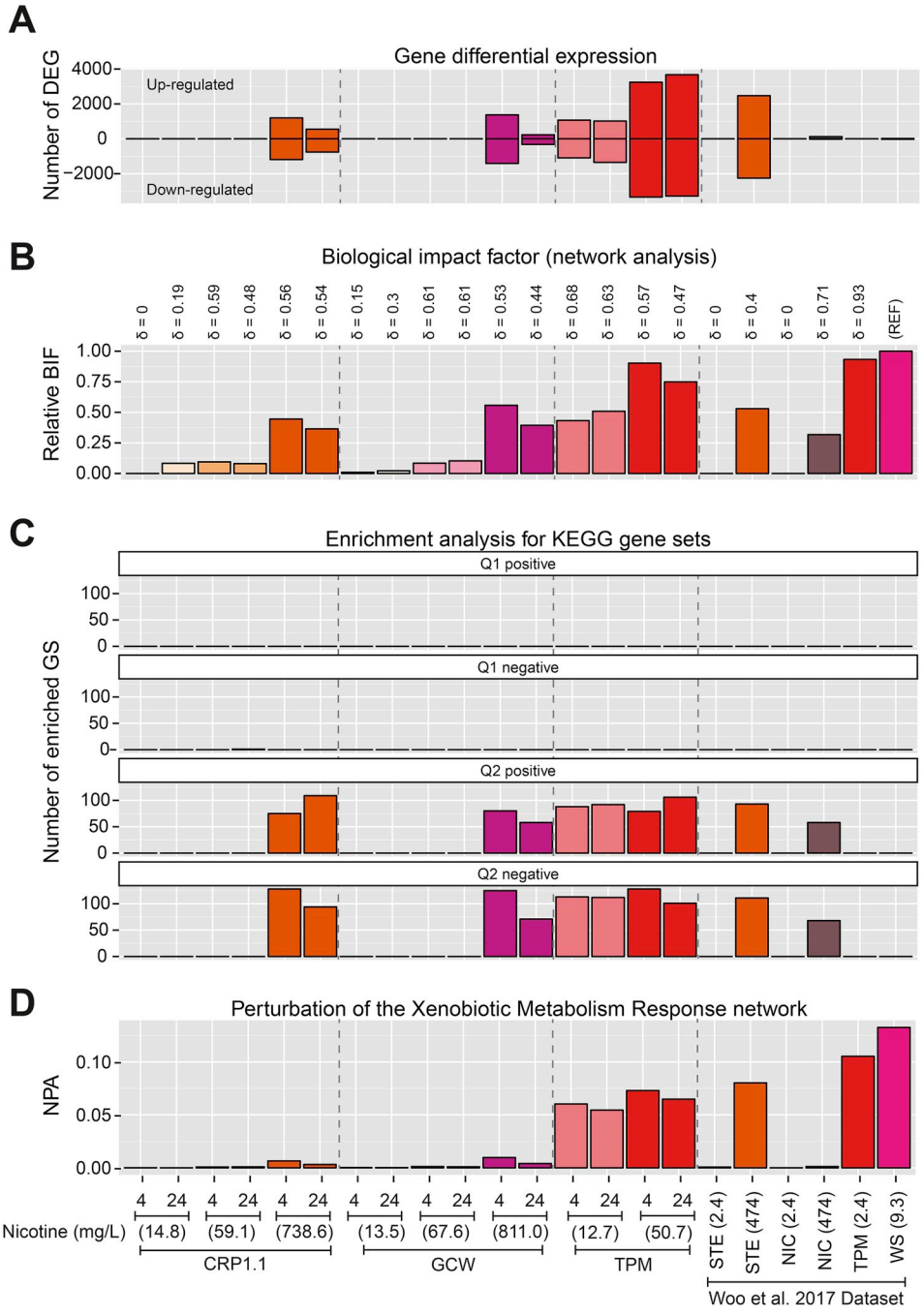

Fig. 7. Gene set comparison with the Woo et al., (2017) dataset. The raw data were downloaded from the GEO website (accession = GSE89923) and reprocessed exactly as the transcriptomics data of our study (see the Materials and Methods). The resulting multiple-part figure enables a comparison of the biological impacts from different but complementary points of view. (**A**) Gene-level: numbers of differentially expressed mRNAs (DEGs) in exposed gingival cultures relative to sham-exposed controls. (**B**) Overall network-level: RBIF, similar to Fig. 3A, which quantifies the global impact in the context of the biology contained in the network models. The δ values above the bars indicate the similarity of the underlying network perturbations to the reference treatment "REF". (**C**) Overall gene set level: numbers of enriched KEGG gene sets according to the GSA score signs and statistics (the self-contained Q2 results are more appropriate for between-treatment comparisons, see the Materials and Methods). (**D**) Biologically relevant NPA of the *Xenobiotic Metabolism Response* network. Times represented (4, 24) refer to hours PE. Concentrations are indicated in parentheses (mg nicotine/L). Abbreviations: BIF, biological impact factor; CRP1.1, CORESTA Reference Product 1.1; DEG, differentially expressed genes; GCW, General Classic White; GS, gene set; KEGG, Kyoto Encyclopedia of Genes and Genomes; NIC, nicotine; NPA, network perturbation amplitude; STE, smokeless tobacco extract (American-type reference moist snuff); TPM, total particulate matter; WS, whole smoke. N = 8–9 for the Zanetti et al. dataset, N = 3 for the Woo et al. dataset.

5. Limitations of the study

This study employs gingival organotypic cultures, which are the state-of-the-art model for *in vitro* research. However, the cultures used in this study are composed entirely of keratinocytes; therefore, the responses to the stimuli are mediated solely by this single cell type. Moreover, the use of cultures derived from a single donor allows for a better experimental reproducibility but may mask donor-specific factors, such as genetic variations. However, in one of our previous studies, Iskandar et al. (2017b) showed with a systems toxicology approach that in bronchial organotypic cultures from two different donors the basic responses to cigarette smoke were quite reproducible; this suggests a common pattern of response to tobacco products between different donors.

As discussed, the different solvents and preparation methods make the direct comparison of the effects of snus extracts and TPM challenging. The extraction protocol used for snus and the exposure of cells to snus high concentrations ensure a situation as close as possible to human consumption; TPM, instead, contains only a fraction of the constituents of cigarette smoke, such as nicotine, polycyclic aromatic hydrocarbons, and TSNAs, but not most volatile compounds, as carbonyls and reactive oxygen species, present instead in the gas vapor phase. In future studies, comparison of liquid snus extract exposure with direct cigarette smoke exposure at the air-liquid interface (Zanetti et al., 2017) can support more relevant comparisons for the human situation.

The replacement of the snus treatment was performed every 24 h for a continuous 72-hour exposure. This exposure regimen does not resemble that of snus users, which is on average around 11–12 h per day (Digard et al., 2009).

Finally, the selection of 50% and 60% as maximum concentrations for the snus extracts (CRP1.1 and GCW, respectively) may not fully cover the high toxicological stimulus range, but it ensures that the molecular modifications observed are driven by toxicity-related mechanisms associated with exposure rather than overt morphological alterations associated with damaged tissues. This approach is in line with the systems toxicology paradigm.

6. Conclusions

At concentrations relevant for snus use in humans, snus extracts from CRP1.1 and GCW exerted similar biological effects on the gingival cultures, e.g. a minimal impact on the cellular morphology. The alterations observed in the gene expression networks in response to snus exposure generally tended to revert with time. While high-concentration snus extract and low-concentration TPM exposure were associated with similar network responses, the xenobiotic metabolism network was less impacted by snus extract, with minimally upregulated *CYP1A1* and *CYP1B1*.

For the first time, to our knowledge, the biological effects of snus were investigated by integrating the miRNA profiles with transcriptomics data, showing 1) that a consistently lower number of miRNAs were altered in gingival cultures by snus extract exposure while the positive control, TPM, exerted a marked response; and 2) identification of high-confidence miRNAs (i.e. mir-125b-5p) that might be related to pathological conditions *in vivo*.

Finally, our data highlight the importance of a network-based analysis by investigating the transcriptomics gene set by Woo et al. with our systems toxicology approach, showing a previously undetected network response to TPM.

Declaration of interest

All authors are employees of, or are contracted (W. K. Schlage) and paid by, Philip Morris International. Philip Morris International is the sole source of funding and sponsor of this project.

Acknowledgements

The authors would like to thank Nicholas Karoglou, Dr. Elena Scotti and Dr. Karsta Luettich for the revision of the manuscript; Laura Ortega Torres for the maintenance of organotypic cultures; Didier Goedertier and Claudius Pak for the TPM and snus extraction; Quentin Dutertre and Sandra Sendyk for nicotine measurements; Dr. Gerhard Lang and Damien de Palo for the TSNA measurements; Sam Ansari, David Bornand, Rémi Dulize, Dariusz Peric, and Karine Baumer for RNA sample processing and transcriptomics data generation; Céline Merg and Maica Corciulo for the inflammatory mediator measurements; Marie Sgandurra and Anaelle Dubois for histological processing; and Dr. Mark Wilsher (Unilabs, London, UK) for histopathological analysis of the organotypic culture models.

Part of this work was presented at the 57th Annual Meeting of the Society of Toxicology in San Antonio, TX, USA, 11–15 March 2018.

Appendix A. Supplementary data

Supplementary data to this article can be found online at https://doi.org/10.1016/j.fct.2018.12.056.

Transparency document

Transparency document related to this article can be found online at https://doi.org/10.1016/j.fct.2018.12.056

References

Ackermann, M., Strimmer, K., 2009. A general modular framework for gene set enrichment analysis. BMC Bioinf. 10, 47.

Affymetrix miRNA QCT Tool, 2011. Affymetrix miRNA QCTool: user's guide. Available at: http://media.affymetrix.com/support/downloads/manuals/mirna_qctool_user_manual.pdf.

Andersen, M.E., Krewski, D., 2009. Toxicity testing in the 21st century: bringing the vision to life. Toxicol. Sci. : an official journal of the Society of Toxicology 107, 324–330.

Asplund, K., Nasic, S., Janlert, U., Stegmayr, B., 2003. Smokeless tobacco as a possible risk factor for stroke in men: a nested case-control study. Stroke 34, 1754–1759.

Barros, S.P., Williams, R., Offenbacher, S., Morelli, T., 2016. Gingival crevicular fluid as a source of biomarkers for periodontitis. Periodontol 2000 70, 53–64.

Benjamini, Y., Hochberg, Y., 1995. Controlling the false discovery rate: a practical and powerful approach to multiple testing. J. Roy. Stat. Soc. B 289–300.

Bergstrom, J., Keilani, H., Lundholm, C., Radestad, U., 2006. Smokeless tobacco (snuff) use and periodontal bone loss. J. Clin. Periodontol. 33, 549–554.

Bertuccio, P., La Vecchia, C., Silverman, D.T., Petersen, G.M., Bracci, P.M., Negri, E., Li, D., Risch, H.A., Olson, S.H., Gallinger, S., Miller, A.B., Bueno-de-Mesquita, H.B., Talamini, R., Polesel, J., Ghadirian, P., Baghurst, P.A., Zatonski, W., Fontham, E.T., Bamlet, W.R., Holly, E.A., Lucenteforte, E., Hassan, M., Yu, H., Kurtz, R.C., Cotterchio, M., Su, J., Maisonneuve, P., Duell, E.J., Bosetti, C., Boffetta, P., 2011. Cigar and pipe smoking, smokeless tobacco use and pancreatic cancer: an analysis from the International Pancreatic Cancer Case-Control Consortium (PanC4). Ann. Oncol. 22, 1420–1426.

Bolstad, B.M., Irizarry, R.A., Astrand, M., Speed, T.P., 2003. A comparison of normalization methods for high density oligonucleotide array data based on variance and bias. Bioinformatics 19, 185–193.

Borgerding, M.F., Bodnar, J.A., Curtin, G.M., Swauger, J.E., 2012. The chemical composition of smokeless tobacco: a survey of products sold in the United States in 2006 and 2007. Regul. Toxicol. Pharmacol. 64, 367–387.

Boué, S., Talikka, M., Westra, J.W., Hayes, W., Di Fabio, A., Park, J., Schlage, W.K., Sewer, A., Fields, B., Ansari, S., Martin, F., Veljkovic, E., Kenney, R., Peitsch, M.C., Hoeng, J., 2015. Causal Biological Network Database: a Comprehensive Platform of Causal Biological Network Models Focused on the Pulmonary and Vascular Systems. Database.

Brettschneider, J., Collin, F., Bolstad, B.M., Speed, T.P., 2008. Quality assessment for short oligonucleotide microarray data. Technometrics 50, 241–264.

Burgess, K.S., Philips, S., Benson, E.A., Desta, Z., Gaedigk, A., Gaedigk, R., Segar, M.W., Liu, Y., Skaar, T.C., 2015. Age-related changes in MicroRNA expression and pharmacogenes in human liver. Clin. Pharmacol. Ther. 98, 205–215.

Carlens, C., Hergens, M.P., Grunewald, J., Ekbom, A., Eklund, A., Hoglund, C.O., Askling, J., 2010. Smoking, use of moist snuff, and risk of chronic inflammatory diseases. Am. J. Respir. Crit. Care Med. 181, 1217–1222.

Carvalho, B.S., Irizarry, R.A., 2010. A framework for oligonucleotide microarray preprocessing. Bioinformatics 26, 2363–2367.

Catlett, N.L., Bargnesi, A.J., Ungerer, S., Seagaran, T., Ladd, W., Elliston, K.O., Pratt, D., 2013. Reverse causal reasoning: applying qualitative causal knowledge to the interpretation of high-throughput data. BMC Bioinf. 14, 340.

Coggins, C.R., Ballantyne, M., Curvall, M., Rutqvist, L.E., 2012. The in vitro toxicology of Swedish snus. Crit. Rev. Toxicol. 42, 304–313.
CORESTA, 2004. The Rationale and Strategy for Conducting in Vitro Toxicology Testing of Tobacco Smoke.
Costea, D.E., Lukandu, O., Bui, L., Ibrahim, M.J., Lygre, R., Neppelberg, E., Ibrahim, S.O., Vintermyr, O.K., Johannessen, A.C., 2010. Adverse effects of Sudanese toombak vs. Swedish snuff on human oral cells. J. Oral Pathol. Med. 39, 128–140.
Crooks, I., Dillon, D.M., Scott, J.K., Ballantyne, M., Meredith, C., 2013. The effect of long term storage on tobacco smoke particulate matter in in vitro genotoxicity and cytotoxicity assays. Regul. Toxicol. Pharmacol. 65, 196–200.
Dai, M., Wang, P., Boyd, A.D., Kostov, G., Athey, B., Jones, E.G., Bunney, W.E., Myers, R.M., Speed, T.P., Akil, H., Watson, S.J., Meng, F., 2005. Evolving gene/transcript definitions significantly alter the interpretation of GeneChip data. Nucleic Acids Res. 33, e175.
Digard, H., Errington, G., Richter, A., McAdam, K., 2009. Patterns and behaviors of snus consumption in Sweden. Nicotine Tob. Res. 11, 1175–1181.
Feyerabend, C., Higenbottam, T., Russell, M.A., 1982. Nicotine concentrations in urine and saliva of smokers and non-smokers. Br. Med. J. 284, 1002–1004.
Foulds, J., Ramstrom, L., Burke, M., Fagerstrom, K., 2003. Effect of smokeless tobacco (snus) on smoking and public health in Sweden. Tobac. Contr. 12, 349–359.
Gale, N., Digard, H., McAdam, K., 2011. Mouth level exposure time on nicotine and TSNA extraction from snus pouches. In: Poster Presented at the CORESTA Smoke Science and Product Technology Study Groups. Meeting Graz, Austria.
Gao, H., Prasad, G.L., Zacharias, W., 2013. Differential cell-specific cytotoxic responses of oral cavity cells to tobacco preparations. Toxicol. Vitro 27, 282–291.
Gentleman, R.C., Carey, V.J., Bates, D.M., Bolstad, B., Dettling, M., Dudoit, S., Ellis, B., Gautier, L., Ge, Y., Gentry, J., Hornik, K., Hothorn, T., Huber, W., Iacus, S., Irizarry, R., Leisch, F., Li, C., Maechler, M., Rossini, A.J., Sawitzki, G., Smith, C., Smyth, G., Tierney, L., Yang, J.Y., Zhang, J., 2004. Bioconductor: open software development for computational biology and bioinformatics. Genome Biol. 5, R80.
Giannopoulou, C., Cappuyns, I., Mombelli, A., 2003. Effect of smoking on gingival crevicular fluid cytokine profile during experimental gingivitis. J. Clin. Periodontol. 30, 996–1002.
Gill, P., Bhattacharyya, S., McCullough, S., Letzig, L., Mishra, P.J., Luo, C., Dweep, H., James, L., 2017. MicroRNA regulation of CYP 1A2, CYP3A4 and CYP2E1 expression in acetaminophen toxicity. Sci. Rep. 7, 12331.
Gong, J., Zhang, J.P., Li, B., Zeng, C., You, K., Chen, M.X., Yuan, Y., Zhuang, S.M., 2013. MicroRNA-125b promotes apoptosis by regulating the expression of Mcl-1, Bcl-w and IL-6R. Oncogene 32, 3071–3079.
Guentsch, A., Preshaw, P.M., Bremer-Streck, S., Klinger, G., Glockmann, E., Sigusch, B.W., 2008. Lipid peroxidation and antioxidant activity in saliva of periodontitis patients: effect of smoking and periodontal treatment. Clin. Oral Invest. 12, 345–352.
Gustafsson, P.E., Persson, M., Hammarström, A., 2011. Life course origins of the metabolic syndrome in middle-aged women and men: the role of socioeconomic status and metabolic risk factors in adolescence and early adulthood. Ann. Epidemiol. 21, 103–110.
Hai, R., Chu, A., Li, H., Umamoto, S., Rider, P., Liu, F., 2006. Infection of human cytomegalovirus in cultured human gingival tissue. Virol. J. 3, 84.
Hoeng, J., Deehan, R., Pratt, D., Martin, F., Sewer, A., Thomson, T.M., Drubin, D.A., Waters, C.A., de Graaf, D., Peitsch, M.C., 2012. A network-based approach to quantifying the impact of biologically active substances. Drug Discov. Today 17, 413–418.
Hoeng, J., Talikka, M., Martin, F., Sewer, A., Yang, X., Iskandar, A., Schlage, W.K., Peitsch, M.C., 2014. Case study: the role of mechanistic network models in systems toxicology. Drug Discov. Today 19, 183–192.
Hoffmann, D., Adams, J.D., 1981. Carcinogenic tobacco-specific N-nitrosamines in snuff and in the saliva of snuff dippers. Cancer Res. 41, 4305–4308.
Holm, H., Jarvis, M.J., Russell, M.A., Feyerabend, C., 1992. Nicotine intake and dependence in Swedish snuff takers. Psychopharmacology (Berl) 108, 507–511.
Huber, W., Carey, V.J., Gentleman, R., Anders, S., Carlson, M., Carvalho, B.S., Bravo, H.C., Davis, S., Gatto, L., Girke, T., Gottardo, R., Hahne, F., Hansen, K.D., Irizarry, R.A., Lawrence, M., Love, M.I., MacDonald, J., Obenchain, V., Oles, A.K., Pages, H., Reyes, A., Shannon, P., Smyth, G.K., Tenenbaum, D., Waldron, L., Morgan, M., 2015. Orchestrating high-throughput genomic analysis with Bioconductor. Nat. Methods 12, 115–121.
IARC, 2007. Smokeless Tobacco and Some Tobacco-specific N-nitrosamines, vol. 89 IARC Monographs on the Evaluation of Carcinogenic Risks to Humans.
Isaza-Guzmán, D., Cardona-Vélez, N., Gaviria-Correa, D., Martínez-Pabón, M., Castaño-Granada, M., Tobón-Arroyave, S., 2015. Association study between salivary levels of interferon (IFN)-gamma, interleukin (IL)-17, IL-21, and IL-22 with chronic periodontitis. Arch. Oral Biol. 60, 91–99.
Iskandar, A.R., Mathis, C., Martin, F., Leroy, P., Sewer, A., Majeed, S., Kuehn, D., Trivedi, K., Grandolfo, D., Cabanski, M., Guedj, E., Merg, C., Frentzel, S., Ivanov, N.V., Peitsch, M.C., Hoeng, J., 2017a. 3-D nasal cultures: systems toxicological assessment of a candidate modified-risk tobacco product. ALTEX 34, 23–48.
Iskandar, A.R., Mathis, C., Schlage, W.K., Frentzel, S., Leroy, P., Xiang, Y., Sewer, A., Majeed, S., Ortega-Torres, L., Johne, S., Guedj, E., Trivedi, K., Kratzer, G., Merg, C., Elamin, A., Martin, F., Ivanov, N.V., Peitsch, M.C., Hoeng, J., 2017b. A systems toxicology approach for comparative assessment: biological impact of an aerosol from a candidate modified-risk tobacco product and cigarette smoke on human organotypic bronchial epithelial cultures. Toxicol. Vitro 39, 29–51.
Iskandar, A.R., Titz, B., Sewer, A., Leroy, P., Schneider, T., Zanetti, F., Mathis, C., Elamin, A., Frentzel, S., Schlage, W.K., Martin, F., Ivanov, N.V., Peitsch, M.C., Hoeng, J., 2017c. Systems Toxicology Meta-analysis of in Vitro Assessment Studies: Biological Impact of a Candidate Modified-risk Tobacco Product Aerosol Compared with Cigarette Smoke on Human Organotypic Cultures of the Aerodigestive Tract *Toxicology Research*.
Johannsen, A., Susin, C., Gustafsson, A., 2014. Smoking and inflammation: evidence for a synergistic role in chronic disease. Periodontol 2000 64, 111–126.
Kallischnigg, G., Weitkunat, R., Lee, P.N., 2008. Systematic review of the relation between smokeless tobacco and non-neoplastic oral diseases in Europe and the United States. BMC Oral Health 8, 13.
Kanehisa, M., Goto, S., Sato, Y., Kawashima, M., Furumichi, M., Tanabe, M., 2014. Data, information, knowledge and principle: back to metabolism in KEGG. Nucleic Acids Res. 42, D199–D205.
Kauffmann, A., Gentleman, R., Huber, W., 2009. arrayQualityMetrics–a bioconductor package for quality assessment of microarray data. Bioinformatics 25, 415–416.
Kho, H.S., 2014. Understanding of xerostomia and strategies for the development of artificial saliva. Chin. J. Dent. Res. 17, 75–83.
Kim, S.G., Chae, C.H., Cho, B.O., Kim, H.N., Kim, H.J., Kim, I.S., Choi, J.Y., 2006. Apoptosis of oral epithelial cells in oral lichen planus caused by upregulation of BMP-4. J. Oral Pathol. Med. 35, 37–45.
Kogel, U., Gonzalez Suarez, I., Xiang, Y., Dossin, E., Guy, P.A., Mathis, C., Marescotti, D., Goedertier, D., Martin, F., Peitsch, M.C., Hoeng, J., 2015. Biological impact of cigarette smoke compared to an aerosol produced from a prototypic modified risk tobacco product on normal human bronchial epithelial cells. Toxicol. Vitro 29, 2102–2115.
Kozomara, A., Griffiths-Jones, S., 2014. miRBase: annotating high confidence microRNAs using deep sequencing data. Nucleic Acids Res. 42, 68–73.
Laytragoon-Lewin, N., Bahram, F., Rutqvist, L.E., Turesson, I., Lewin, F., 2011. Direct effects of pure nicotine, cigarette smoke extract, Swedish-type smokeless tobacco (Snus) extract and ethanol on human normal endothelial cells and fibroblasts. Anticancer Res. 31, 1527–1534.
Lee, J., Taneja, V., Vassallo, R., 2012. Cigarette smoking and inflammation: cellular and molecular mechanisms. J. Dent. Res. 91, 142–149.
Lee, P.N., 2011. Summary of the epidemiological evidence relating snus to health. Regul. Toxicol. Pharmacol. 59, 197–214.
Lee, P.N., 2013a. The effect on health of switching from cigarettes to snus - a review. Regul. Toxicol. Pharmacol. 66, 1–5.
Lee, P.N., 2013b. Epidemiological evidence relating snus to health–an updated review based on recent publications. Harm Reduct. J. 10, 36.
Lewin, F., Norell, S.E., Johansson, H., Gustavsson, P., Wennerberg, J., Biorklund, A., Rutqvist, L.E., 1998. Smoking tobacco, oral snuff, and alcohol in the etiology of squamous cell carcinoma of the head and neck: a population-based case-referent study in Sweden. Cancer 82, 1367–1375.
Liberzon, A., 2014. A description of the molecular signatures database (MSigDB) web site. Methods Mol. Biol. 1150, 153–160.
Liberzon, A., Subramanian, A., Pinchback, R., Thorvaldsdóttir, H., Tamayo, P., Mesirov, J.P., 2011. Molecular signatures database (MSigDB) 3.0. Bioinformatics 27, 1739–1740.
Malpass, G.E., Arimilli, S., Prasad, G.L., Howlett, A.C., 2013. Complete artificial saliva alters expression of proinflammatory cytokines in human dermal fibroblasts. Toxicol. Sci. 134, 18–25.
Malpass, G.E., Arimilli, S., Prasad, G.L., Howlett, A.C., 2014. Regulation of gene expression by tobacco product preparations in cultured human dermal fibroblasts. Toxicol. Appl. Pharmacol. 279, 211–219.
Martin, F., Sewer, A., Talikka, M., Xiang, Y., Hoeng, J., Peitsch, M., 2014. Quantification of biological network perturbations for mechanistic insight and diagnostics using two-layer causal models. BMC Bioinf. 15, 238.
Martin, F., Thomson, T.M., Sewer, A., Drubin, D.A., Mathis, C., Weisensee, D., Pratt, D., Hoeng, J., Peitsch, M.C., 2012. Assessment of network perturbation amplitudes by applying high-throughput data to causal biological networks. BMC Syst. Biol. 6, 54.
McCall, M.N., Bolstad, B.M., Irizarry, R.A., 2010. Frozen robust multiarray analysis (fRMA). Biostatistics 11, 242–253.
Merne, M., Heikinheimo, K., Saloniemi, I., Syrjanen, S., 2004. Effects of snuff extract on epithelial growth and differentiation in vitro. Oral Oncol. 40, 6–12.
Merne, M., Heinaro, I., Lahteenoja, H., Syrjanen, S., 2002. Proliferation and differentiation markers in snuff-induced oral mucosal lesions. J. Oral Pathol. Med. 31, 259–266.
Modeer, T., Lavstedt, S., Ahlund, C., 1980. Relation between tobacco consumption and oral health in Swedish schoolchildren. Acta Odontol. Scand. 38, 223–227.
Moharamzadeh, K., Franklin, K.L., Brook, I.M., van Noort, R., 2009. Biologic assessment of antiseptic mouthwashes using a three-dimensional human oral mucosal model. J. Periodontol. 80, 769–775.
Morelli, E., Leone, E., Cantafio, M.E., Di Martino, M.T., Amodio, N., Biamonte, L., Gulla, A., Foresta, U., Pitari, M.R., Botta, C., Rossi, M., Neri, A., Munshi, N.C., Anderson, K.C., Tagliaferri, P., Tassone, P., 2015. Selective targeting of IRF4 by synthetic microRNA-125b-5p mimics induces anti-multiple myeloma activity in vitro and in vivo. Leukemia 29, 2173–2183.
Mulhall, H.J., Hughes, M.P., Kazmi, B., Lewis, M.P., Labeed, F.H., 2013. Epithelial cancer cells exhibit different electrical properties when cultured in 2D and 3D environments. Biochim. Biophys. Acta 1830, 5136–5141.
NRC, 2007. Toxicity Testing in the 21st Century: a Vision and a Strategy. National Research Council. National Academies Press.
Ozcaka, O., Bicakci, N., Pussinen, P., Sorsa, T., Kose, T., Buduneli, N., 2011. Smoking and matrix metalloproteinases, neutrophil elastase and myeloperoxidase in chronic periodontitis. Oral Dis. 17, 68–76.
Persson, P.G., Carlsson, S., Svanström, L., Östenson, C.G., Efendic, S., Grill, V., 2000. Cigarette smoking, oral moist snuff use and glucose intolerance. J. Intern. Med. 248, 103–110.
Persson, P.G., Hellers, G., Ahlbom, A., 1993. Use of oral moist snuff and inflammatory bowel disease. Int. J. Epidemiol. 22, 1101–1103.
Popat, R.V., Bhavsar, N.V., Popat, P.R., 2014. Gingival crevicular fluid levels of Matrix Metalloproteinase-1 (MMP-1) and Tissue Inhibitor of Metalloproteinase-1 (TIMP-1)

in periodontal health and disease. Singapore Dent. J. 35, 59–64.
Preetha, A., Banerjee, R., 2005. Comparison of artificial saliva substitutes. Trends Biomater. Artif. Organs 18 (2).
Puy, C.L., 2006. The role of saliva in maintaining oral health and as an aid to diagnosis. Med. Oral Patol. Oral Cir. Bucal 11, 449–455.
R Core Team, 2013. R: a Language and Environment for Statistical Computing. R Foundation for Statistical Computing, Vienna, Austria Available at: http://www.R-project.org/.
Ramstrom, L., Borland, R., Wikmans, T., 2016. Patterns of smoking and snus use in Sweden: implications for public health. Int. J. Environ. Res. Publ. Health 13.
Rathnayake, N., Åkerman, S., Klinge, B., Lundegren, N., Jansson, H., Tryselius, Y., Sorsa, T., Gustafsson, A., 2013. Salivary biomarkers of oral health–a cross-sectional study. J. Clin. Periodontol. 40, 140–147.
Robson, N., Bond, A., Wolff, K., 2010. Salivary Nicotine and Cotinine Concentrations in Unstimulated and Stimulated Saliva.
Roosaar, A., Johansson, A.L., Sandborgh-Englund, G., Nyren, O., Axell, T., 2006. A long-term follow-up study on the natural course of snus-induced lesions among Swedish snus users. Int. J. Canc. 119, 392–397.
Ru, Y., Kechris, K.J., Tabakoff, B., Hoffman, P., Radcliffe, R.A., Bowler, R., Mahaffey, S., Rossi, S., Calin, G.A., Bemis, L., Theodorescu, D., 2014. The multiMiR R package and database: integration of microRNA-target interactions along with their disease and drug associations. Nucleic Acids Res. 42, e133.
Rutqvist, L.E., Curvall, M., Hassler, T., Ringberger, T., Wahlberg, I., 2011. Swedish snus and the GothiaTek(R) standard. Harm Reduct. J. 8, 11.
Sapna, G., Gokul, S., Bagri-Manjrekar, K., 2014. Matrix metalloproteinases and periodontal diseases. Oral Dis. 20, 538–550.
Sauer, J.M., Kleensang, A., Peitsch, M.C., Hayes, A.W., 2016. Advancing risk assessment through the application of systems toxicology. Toxicol Res 32, 5–8.
Schlage, W.K., Iskandar, A.R., Kostadinova, R., Xiang, Y., Sewer, A., Majeed, S., Kuehn, D., Frentzel, S., Talikka, M., Geertz, M., Mathis, C., Ivanov, N., Hoeng, J., Peitsch, M.C., 2014. In vitro systems toxicology approach to investigate the effects of repeated cigarette smoke exposure on human buccal and gingival organotypic epithelial tissue cultures. Toxicol. Mech. Methods 24, 470–487.
Seeman, J.I., Lipowicz, P.J., Piade, J.J., Poget, L., Sanders, E.B., Snyder, J.P., Trowbridge, C.G., 2004. On the deposition of volatiles and semivolatiles from cigarette smoke aerosols: relative rates of transfer of nicotine and ammonia from particles to the gas phase. Chem. Res. Toxicol. 17, 1020–1037.
Seidenberg, A.B., Ayo-Yusuf, O.A., Rees, V.W., 2016. Characteristics of “American Snus” and Swedish Snus Products for Sale in Massachusetts, USA. Nicotine & Tobacco Research, pp. ntw334.
Semlali, A., Witoled, C., Alanazi, M., Rouabhia, M., 2012. Whole cigarette smoke increased the expression of TLRs, HBDs, and proinflammory cytokines by human gingival epithelial cells through different signaling pathways. PLoS One 7, e52614.
Smyth, G.K., 2004. Linear models and empirical bayes methods for assessing differential expression in microarray experiments. Stat. Appl. Genet. Mol. Biol. 3, 3.
Steiling, K., Ryan, J., Brody, J.S., Spira, A., 2008. The Field of Tissue Injury in the Lung and Airway, vol. 1. Cancer prevention research, Philadelphia, Pa, pp. 396–403.
Stepanov, I., Villalta, P.W., Knezevich, A., Jensen, J., Hatsukami, D., Hecht, S.S., 2010. Analysis of 23 polycyclic aromatic hydrocarbons in smokeless tobacco by gas chromatography-mass spectrometry. Chem. Res. Toxicol. 23, 66–73.
Stratton, K., Shetty, P., Wallace, R., Bondurant, S., 2001. Clearing the smoke: the science base for tobacco harm reduction—executive summary. Tobac. Contr. 10, 189–195.
Sturla, S.J., Boobis, A.R., FitzGerald, R.E., Hoeng, J., Kavlock, R.J., Schirmer, K., Whelan, M., Wilks, M.F., Peitsch, M.C., 2014. Systems toxicology: from basic research to risk assessment. Chem. Res. Toxicol. 27, 314–329.
Thomson, T.M., Sewer, A., Martin, F., Belcastro, V., Frushour, B.P., Gebel, S., Park, J., Schlage, W.K., Talikka, M., Vasilyev, D.M., Westra, J.W., Hoeng, J., Peitsch, M.C., 2013. Quantitative Assessment of Biological Impact Using Transcriptomic Data and Mechanistic Network Models. Toxicology and Applied Pharmacology.
Tsang, S.M., Brown, L., Lin, K., Liu, L., Piper, K., O'Toole, E.A., Grose, R., Hart, I.R., Garrod, D.R., Fortune, F., Wan, H., 2012. Non-junctional human desmoglein 3 acts as an upstream regulator of Src in E-cadherin adhesion, a pathway possibly involved in the pathogenesis of pemphigus vulgaris. J. Pathol. 227, 81–93.
Turabelidze, A., Guo, S., Chung, A.Y., Chen, L., Dai, Y., Marucha, P.T., DiPietro, L.A., 2014. Intrinsic differences between oral and skin keratinocytes. PLoS One 9, e101480.
van Roy, F., Berx, G., 2008. The cell-cell adhesion molecule E-cadherin. Cell. Mol. Life Sci. 65, 3756–3788.
Varemo, L., Nielsen, J., Nookaew, I., 2013. Enriching the gene set analysis of genome-wide data by incorporating directionality of gene expression and combining statistical hypotheses and methods. Nucleic Acids Res. 41, 4378–4391.
Wang, Y., Rotem, E., Andriani, F., Garlick, J.A., 2001. Smokeless tobacco extracts modulate keratinocyte and fibroblast growth in organotypic culture. J. Dent. Res. 80, 1862–1866.
Wedenberg, C., Jonsson, A., Hirsch, J.M., 1996. Assessment of p53 and Ki-67 expression in snuff-induced lesions. Br. J. Oral Maxillofac. Surg. 34, 409–413.
Woo, S., Gao, H., Henderson, D., Zacharias, W., Liu, G., Tran, Q.T., Prasad, G.L., 2017. AKR1C1 as a Biomarker for Differentiating the Biological Effects of Combustible from Non-combustible Tobacco Products. Genes 8.
Wood, M.W., Medina, J.E., Thompson, G.C., Houck, J.R., Min, K.W., 1994. Accumulation of the p53 tumor-suppressor gene product in oral leukoplakia. Otolaryngol. Head Neck Surg. 111, 758–763.
Wu, D., Lim, E., Vaillant, F., Asselin-Labat, M.L., Visvader, J.E., Smyth, G.K., 2010. ROAST: rotation gene set tests for complex microarray experiments. Bioinformatics 26, 2176–2182.
Wu, D., Smyth, G.K., 2012. Camera: a competitive gene set test accounting for inter-gene correlation. Nucleic Acids Res. 40, e133.
Zanetti, F., Sewer, A., Mathis, C., Iskandar, A.R., Kostadinova, R., Schlage, W.K., Leroy, P., Majeed, S., Guedj, E., Trivedi, K., Martin, F., Elamin, A., Merg, C., Ivanov, N.V., Frentzel, S., Peitsch, M.C., Hoeng, J., 2016. Systems toxicology assessment of the biological impact of a candidate modified risk tobacco product on human organotypic oral epithelial cultures. Chem. Res. Toxicol. 29, 1252–1269.
Zanetti, F., Sewer, A., Scotti, E., Titz, B., Schlage, W.K., Leroy, P., Kondylis, A., Vuillaume, G., Iskandar, A.R., Guedj, E., Trivedi, K., Schneider, T., Elamin, A., Martin, F., Frentzel, S., Ivanov, N.V., Peitsch, M.C., Hoeng, J., 2018. Assessment of the impact of aerosol from a potential modified risk tobacco product compared with cigarette smoke on human organotypic oral epithelial cultures under different exposure regimens. Food Chem. Toxicol. 115, 148–169.
Zanetti, F., Titz, B., Sewer, A., Lo Sasso, G., Scotti, E., Schlage, W.K., Mathis, C., Leroy, P., Majeed, S., Torres, L.O., Keppler, B.R., Elamin, A., Trivedi, K., Guedj, E., Martin, F., Frentzel, S., Ivanov, N.V., Peitsch, M.C., Hoeng, J., 2017. Comparative systems toxicology analysis of cigarette smoke and aerosol from a candidate modified risk tobacco product in organotypic human gingival epithelial cultures: a 3-day repeated exposure study. Food Chem. Toxicol. 101, 15–35.